CHALMERS
UNIVERSITY OF TECHNOLOGY

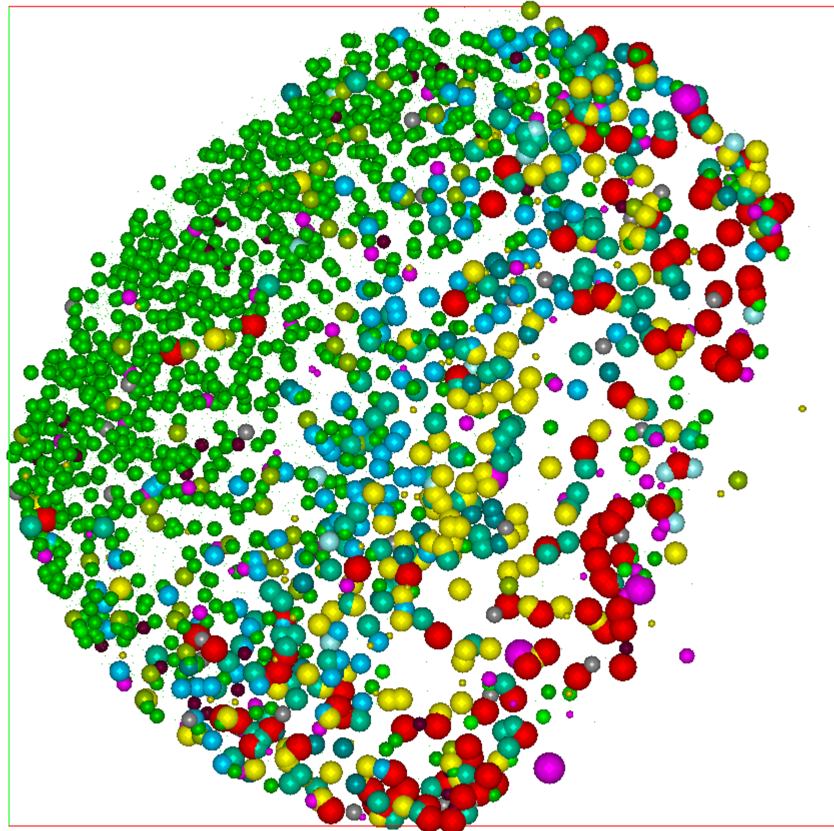

Fabrication of silica on silicon tips for protein analysis using Atom Probe Tomography

Master's thesis in Nanotechnology

SAIEESH VIJAYENDRA NAYAK

DEPARTMENT OF CHEMISTRY AND CHEMICAL ENGINEERING

CHALMERS UNIVERSITY OF TECHNOLOGY
Gothenburg, Sweden 2022
www.chalmers.se

Fabrication of silica on silicon tips for protein analysis using Atom Probe Tomography
Saieesh Nayak

© SAIEESH VIJAYENDRA NAYAK, 2022.

Supervisors: Martin Andersson, Mats Hulander, Department at Chemistry and Chemical Engineering, Chalmers University of Technology
PhD Supervisor: Gustav Eriksson, Chalmers University of Technology
Examiner: Martin Andersson, Deputy Head of Department at Chemistry and Chemical Engineering, Chalmers University of Technology

Master's Thesis 2022
Department at Chemistry and Chemical Engineering
Department at Microtechnology and Nanoscience
Martin Andersson research group
Chalmers University of Technology
SE-412 96 Gothenburg
Telephone +46 31 772 1000

Cover: Reconstructed Image of Nickel tip from Atom Probe Tomography data

Typeset in LaTeX
Printed by Chalmers Reproservice
Gothenburg, Sweden 2022

Abstract

This report appraises the custom wet etching technique using Hydrofluoric acid and potassium hydroxide as etchant on silica on silicon chip to prepare Atom Probe Tomography tips. In addition, the report includes how different novel techniques can be used for evaluating the wet etched APT specimen's potential to be adapted for protein analysis, such as Atom Probe Tomography (APT) and Quartz Crystal Microbalance-Dissipation (QCM-D).

Furthermore, it explains the procedure of fabricating Atom probe tips using electropolishing of Nickel and Tungsten wires along with sputter coating of different metals such as Gold and Chromium on the surface for analysis in the Atom Probe Tomography. Subsequently, it presents several images of electropolished tips which were captured using a Scanning Electron Microscope to determine the thickness of the sputtered metal (Au/Cr).

It also describes in detail, the usage of K-Layout software for designing an array of circles with different diameters. This design was used as a pattern during the exposure in the Electron Beam Lithography. It also appraises the different instruments used such as electropolishing, sputter coater, cleanroom facility, Electron Beam Lithography, and Scanning Electron Microscope, which was used to fabricate and image the samples fabricated, during the project and its principle for understanding the reason of methodology.

Keywords: Atom Probe Tomography, Wet etching, Quartz Crystal Microbalance-Dissipation, Electropolishing, Sputter coating, Scanning Electron Microscope.

Acknowledgements

First and foremost, I would like to thank my supervisors and examiner Martin Andersson, and Mats Hulander for the opportunity to execute my master's thesis at the department, and for the opportunity to learn about different techniques and instruments at the Chalmers University of Technology. I would also like to thank all the people at Martin Andersson's research group for your contributions to this diploma work and the warm welcome.

I am very grateful and would like to thank Karin Hedsten, Peter Modh, Ruggero Verre, and John Halonen for their assistance and guidance with the project at every step. A special thank you to Gustav Sundell for guiding and helping me with the initial stage of my project. A huge thank you to Mattias Thuvander for all the help, guidance, and input, for the completion of the project.

The greatest of thanks to my Ph.D. supervisor Gustav Eriksson, for all your encouragement and support during the whole project. Thank you very much for being there to help me clarify my doubts and rectify my mistakes and for making time to discuss any questions. The help I have received from you has been indispensable.

A sincere appreciation towards Chalmers Materials Analysis Laboratory facilities and Cleanroom at MC2. My deepest gratitude towards Niclas Lindvall for guiding and helping me through my master's project in the clean room and with Electron Beam Lithography. I would also like to thank all the people at MC2 Department, Chemistry and Chemical Engineering Department, cleanroom faculties, and CMAL faculties for your contributions to this diploma work and the warm welcome.

Finally, my sincerest thank you to my family for their constant love and support throughout my years at the Chalmers University of Technology.

List of Acronyms

Below is the list of acronyms that have been used throughout this thesis listed in alphabetical order:

Abbreviation	Fullform
AH	Aluminium Holder
APT	Atom Probe Tomography
EBL	Electron Beam Lithography
EP	Electropolishing
QCMD	Quartz Crystal Microbalance -Dissipation
ROI	Region of Interest
SEM	Scanning Electron Microscope

Contents

List of Acronyms **vii**

List of Figures **xi**

List of Tables **xiii**

1 Introduction **1**
1.1 Background 1
1.2 Purpose 2

2 Theory **3**
2.1 Electropolishing 3
2.2 Sputter coating 4
2.3 Scanning Electron Microscope 6
2.4 Atom Probe Tomography 7
2.5 Quartz Crystal Microbalance-Dissipation 7
2.6 Electron Beam Lithography 8
2.7 Cleanroom facility 9

3 Methods **11**
3.1 Electropolishing 11
3.2 Sputter coater 12
3.3 Fabrication of Silica chip 13
3.3.1 Hydrofluoric acid etching of silica 15
3.3.2 Potassium Hydroxide etching of silicon 15
3.4 QCMD 15
3.5 Atom Probe Tomography 16

4 Results **17**
4.1 Electropolishing and sputter coating 17
4.2 Wet etching of silica on silicon chip 17
4.3 Imaging of samples 18
4.4 Atom Probe Tomography 19

5 Conclusion **31**
5.1 Future Work 32

Bibliography **33**

A Appendix 1 **I**

List of Figures

2.1 The voltage/current density curve for a typical electropolishing solution. Electropolishing is typically performed within the plateau (BC) region of the curve. 3
2.2 Schematic image of electropolishing process 4
2.3 Schematic image of sputter-coating 5
2.4 Image of Leica sputter coater 5
2.5 Image of Zeiss Ultra 55 SEM 6
2.6 Schematic of SEM 6
2.7 Image of Atom Probe Tomograph instrument 7
2.8 Image of QCMD instrument 8
2.9 Image of EBL JEOL JBX 9300FS 9

3.1 Electropolishing setup with AC supply 11
3.2 Nickel tip 12
3.3 Tungsten tip 12
3.4 Time versus thickness plot 13
3.5 Design of pattern in K Layout 14
3.6 Image of silica on silicon chip after EBL array design 15

4.1 Image of surface after HF and KOH etching 18
4.2 Image of 110 nanometers etched on the surface 19
4.3 Image of 110 nanometers etched on the surface at 30 ° 20
4.4 Image of 110 nanometers etched on surface at 30 °and 10kX zoom . . 21
4.5 Image of the angle formed of 110 nanometers etched on the surface at 30 ° 22
4.6 Image of etched height of 110 nanometers etched on the surface at 30° 23
4.7 Nickel tip 23
4.8 Gold sputtered Nickel tip 24
4.9 Nickel tip 24
4.10 Gold sputtered Nickel tip 25
4.11 Tungsten tip 25
4.12 Gold sputtered Tungsten tip 26
4.13 Spatial distribution in ROI of Ni-Au tip 26
4.14 Legend representing the detected ions in the mass spectrum during image reconstruction 27
4.15 2D contour of the oxide layer in Ni-Au tip ROI 27
4.16 Cross sectional image of Ni Au tip 28

4.17 Mass spectrum of Ni-Au tip on logarithmic scale 28
4.18 Mass spectrum of Ni-Au tip 29

A.1 301X Magnification with measurement for 210 nm diameter pattern . II
A.2 433X Magnification with measurement for 210 nm diameter pattern . II
A.3 30KX Magnification with measurement for 210 nm diameter pattern . III
A.4 30KX Magnification with measurement for 210 nm diameter pattern . III
A.5 22KX Magnification with measurement for 250 nm diameter pattern at 550 dosage IV
A.6 Image of surface of silica on silicon chip after HF and KOH etching . IV
A.7 Image of 400 nm etched circle near 110 nm text IV

List of Tables

2.1 Simplified ISO classes (maximum level of particles /m^3) 9

1

Introduction

1.1 Background

Proteins are complex macromolecules that build up most of life. A chain of amino acids constructs them, and many of these sequences are known. The chain-folds form a specific 3D structure which distinctly determines the protein's physical properties, interactions and functionality. Determination of the 3D structure of the protein molecule is vital as the protein function depends on its 3D structure. Some empirical methods determine the 3D structure of proteins, such as Nuclear Magnetic Resonance (NMR) and X-Ray Diffraction (XRD). Novel methods include the use of cryo-electron microscopy (Cryo-EM) [1]. These methods have their advantages and limitations. Therefore other proteins have been approximated by calculation. Still, this remains an unsolved and critical problem [2].

Large proteins are traditionally examined by X-ray crystallography which requires crystallisation of the protein. The crystallisation is a complicated process, and it usually takes months to years to find appropriate conditions for a specific protein. Smaller proteins are typically determined with nuclear magnetic resonance combined with existing sequence information. Therefore, this method does not require crystallisation and is more favourable in time consumption. The issue is that larger molecules can not be examined due to technical limitations while using the NMR technique [2].

Atom Probe Tomography (APT) is an analysis technique used to analyse the 3D structure of the sample as well as its chemical composition measurements near-atomic scale. It has a resolution of approximately 0.1-0.3nm in-depth, and 0.3-0.5nm laterally [2]. The sample to be analysed in the APT must be in the form of a tip whose apex of the tip is sub 100 nanometers in diameter. The tip is placed on a "holder" inside the APT chamber. A high field is applied across the end of the sample tip. It runs on two modes which are pulsed voltage mode and laser mode. The field evaporation can be achieved by either laser pulsing through thermal assistance or voltage pulsing through field assistance. The reason for pulsing is to achieve field evaporation to occur at only set time points to measure the time of field correctly. In laser pulsing mode, the atoms undergo field evaporation when the laser excites the particular atom under the applied field's influence, just below its threshold of field evaporation. The specimen will temporarily be pushed above this threshold due to energy from the laser. Subsequently, in the voltage pulsing method, the applied field

is increased by a set percentage. This field puts the specimen above the threshold for making field evaporation of the atoms likely enough to get a good evaporation rate. These ions travel to the detector. The time of flight and the location of the ion detection event on the position-sensitive detector are determined. This data is later reconstructed for its 3D configuration, and ions are analysed in the mass spectrum detected on the detector[3].

The size limitation holds well for analysing protein using Atom Probe Tomography. The average size of a protein molecule is 149 nm, with a standard deviation of 56.5 nm [4]. The sample tip used for analysis must be in the sub 100 nm range. Hence various methods of fabricating the tip have to be studied. Focused Ion Beam Scanning Electron Microscopy (FIBSEM) is one of the techniques used widely to prepare APT sample specimen tips. However, this technique is suspected of having caused damage to the sample specimen, due to which FIB-free techniques are of interest in preparing the APT sample specimen.

1.2 Purpose

This project introduces a new fabricating method for APT tips with protein embedded in the tip. The protein present in the sample tip gets detected in the APT for further protein analysis. The protein is encapsulated in a silica matrix due to its hydrophobic nature [5]. It also provides the needle-shaped specimen with sufficient mechanical integrity to permit atom probe analysis. Due to the low electrical conductivity of silica, the tips are sputtered with metal which is more conductive and thus can transport the applied potential to the apex of the tip, making the field evaporation easier. Studies were also conducted on the effect of field evaporation due to different sputtering materials on different metal tips.
The project focused on structuring the methodology for preparing good silica on silicon APT tips without embedded proteins, using wet etching techniques. It was achieved using Electron Beam Lithography (EBL) to etch the pattern, which was designed using K Layout software. Successful APT metal tips were fabricated using Electro Polishing(EP) technique. The APT metal tips fabricated using EP and the sputter-coated APT metal tips were analysed in the APT to analyse the field evaporation of metal and sputter-coated metal in the APT.

2
Theory

2.1 Electropolishing

One of the most common methods is fabricating the needle-shaped tips from metallic wires. However, each material has different electropolishing conditions, including composition, temperature and viscosity of the electrolyte and the voltage-current parameters applied to the cell[2]. Figure 2.1 shows a voltage/current density curve for a typical electropolishing solution.

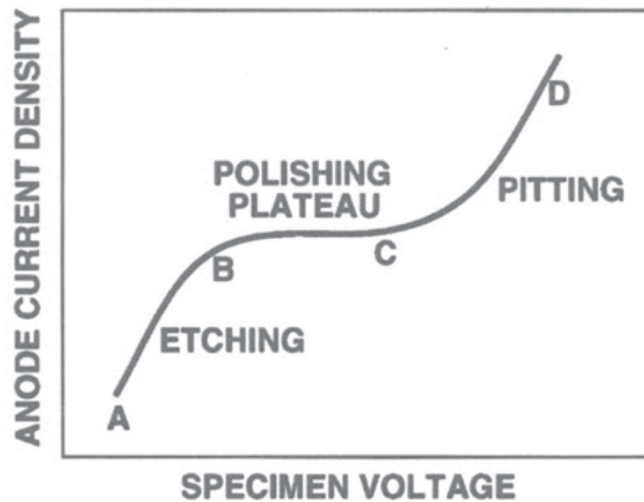

Figure 2.1: The voltage/current density curve for a typical electropolishing solution. Electropolishing is typically performed within the plateau (BC) region of the curve.

The electropolishing process is generally a two-step process. In the first step, the electrolyte is used along with inert fluid. This inert fluid helps terminate the electropolishing process and is used to create a V-shape to have a uniform etching in the electrolyte solution. The second step is usually performed in a simple bath of electrolyte instead of inert fluid for uniform electropolishing in the electrolyte solution. A schematic image of the electropolishing process is shown in the figure 2.6 The curve has been divided into three sections from the schematic diagram, i.e. Low voltage region AB, Polishing plateau BC, and High voltage region CD.In the AB region, the more reactive points on the surface of the needle are favourably attacked. The AB etch region is accepted for not producing a good shiny surface finish. Subsequently, the BC region is known for fabricating the desired smooth,

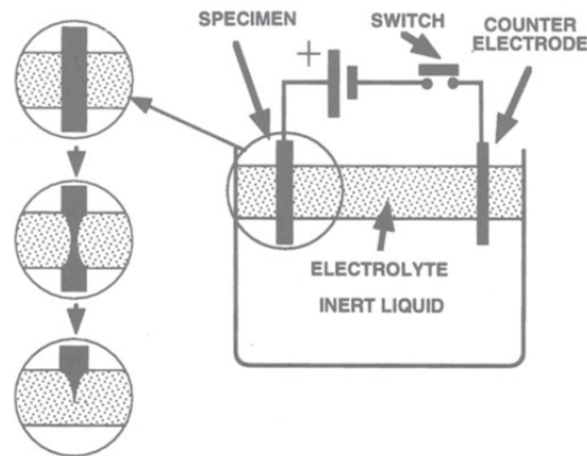

Figure 2.2: Schematic image of electropolishing process

shiny surface finish. In addition, the polishing plateau during electropolishing forms two films on the surface of the specimen tips. A thin solid film of approximately 1 to 10 nm thick is formed on the specimen tips. This film is continuously being dissolved and reformed, and it is the first film. The second film is thicker than the first, approximately a micron thick, that holds a high concentration of ions. This viscous film is visible in the clear electrolyte solutions in the form of a coloured trail from the sample. The majority of the sample tips are polished in this region. Consequently, the CD region is well known for continuing the polishing process along with high current density, partially due to the evolution of gas at the anode during the electropolishing process. This evolved gas caused pits' formation due to the thick film's disruption[2].

2.2 Sputter coating

A Sputter coater is mainly used for producing homogeneous and conductive metal coatings for electron microscopy analysis. The LEICA EM ACE200 was used for performing any sputtering activities. The instrument had an inbuilt option for using the thickness required to be sputtered in the manual or automatic mode. The instrument uses a Quartz crystal to measure the thickness sputtered on the sample tip in the automatic mode. In the manual mode, the current and time parameters have to be set by the operator.

Sputter coating of a sample is a simple process in which an energetic particle bombards a target surface with sufficient energy to eject one or more atoms from the target. The aspects of sputtering that may lead to significant effects on film deposition are reflected, energetic neutrals, and negative ions [6]. Figure 2.3 represents the schematic image of sputter-coating process.
The instrument measures the thickness sputtered in the automatic mode based on the Quartz Crystal Measurement. The sputter coating process undergoes pumping, purging, pre sputter pressure, sputtering, post-correction and venting. Argon gas

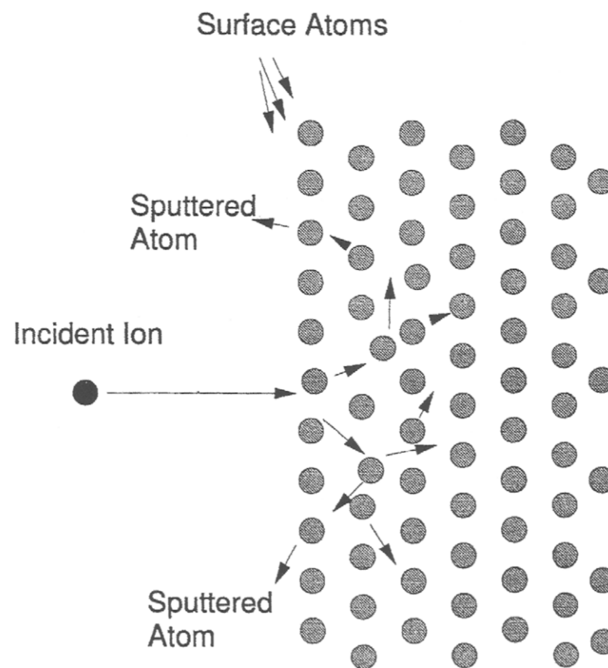

Figure 2.3: Schematic image of sputter-coating

was used for sputtering. Once the desired pressure is achieved, each step is followed in the mentioned manner. The advantage of using this instrument was that the stage tilt option was available. The stage tilt angle was set at -30°, which ensured the uniform sputter coating of Au and Cr on the sample as it was perpendicular to the source. The image of the sputter coating instrument is shown in figure 2.4

Figure 2.4: Image of Leica sputter coater

2.3 Scanning Electron Microscope

Scanning Electron Microscopy (SEM) is one of the types of Electron microscopy techniques, with the other being Transmission Electron Microscope (TEM). The SEM used in the experiment is Zeiss Ultra 55 SEM and is shown in figure 2.5

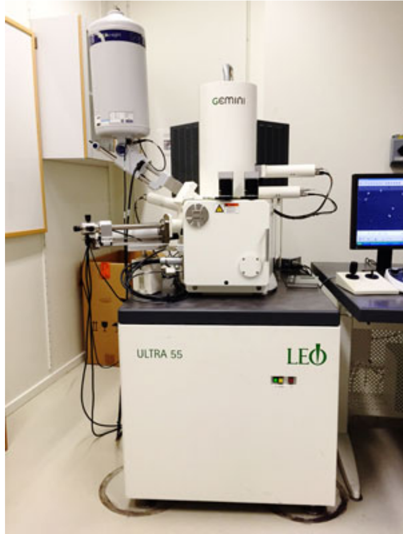

Figure 2.5: Image of Zeiss Ultra 55 SEM

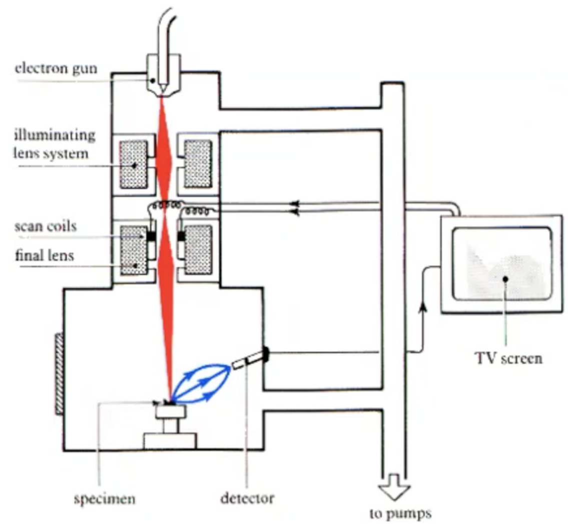

Figure 2.6: Schematic of SEM

SEM uses an electron beam to image the samples with very high resolution down to the nanometer scale. The schematic image of an SEM is shown in figure 2.6. In the electron gun, the filament in the SEM emits electrons either by a thermal emission source, such as a heated tungsten filament or by a field emission cathode. These electrons align with the help of a condenser lens. The condenser lens defines the resolution by defining the size of the electron beam. Subsequently, the electrons pass through the scan coils. The function of the scan coil is to control the position of the electron beam above the objective lens. The coils allow the beam to scan across the surface of the sample. These electrons pass through an objective lens which focuses the beam onto the sample.

The SEM uses secondary electrons (SE) and back scattered electrons (BSE) for image formation. SE that get detected are primarily from the sample's surface, whereas the BSE that get detected are penetrated through the sample's surface. The SE generally gives topographical contrast, while BSE gives more information on the chemical contrast of the sample. The BSE are reflected after elastic interactions between the beam and the sample. The SE are originated from the atoms of the sample on the surface. They result from inelastic interaction between the electron beam and the sample. The SEM X-ray detector also collects characteristics of X-rays generated by electron matter interactions and provides chemical information about the sample. The contrast in a SEM image is due to electron beam-induced current (EBIC) [7]. The amount of electrons detected for each location the electron beam is on is measured and gives a relative contrast to the other measured amounts.

2.4 Atom Probe Tomography

Atom Probe Tomography (APT) is a microscopy technique that provides 3D atom-by-atom imaging of materials and a combination of spatial and chemical resolution. It runs on two modes which are pulsed voltage mode and laser mode. A wide range of materials can be analyzed in the laser pulse mode, including metals, alloys, intermetallics, semiconductors, thin films and oxide scales [2]. The sensitivity is the same for all elements (except for hydrogen), including the light elements like C, O and N. The principle of the APT technique is based on field evaporation of ions from a very sharp needle-shaped sample [3]. Electropolishing is applied to fabricate suitable samples in this project. The volume of analyzed material is about 60 x 60x 200 nm^3, enabling the instrument to detect and chemically identify several million ions. The chemical identification is carried out based on the time of flight calculation. It is analyzed with the help of the mass to charge ratio mass spectrum obtained during image reconstruction. The image of the instrument is shown in figure 2.7

Figure 2.7: Image of Atom Probe Tomograph instrument

The aspect ratio of the APT tips is maintained to be high to achieve high field evaporation[2]. The sample is placed on a holder and is aligned before the analysis. During analysis, an electric field is applied below the threshold of ionisation of atoms. In the laser mode, the laser excites the atoms such that it crosses the threshold of field evaporation and hit the detector. It also scouts for the surface with high field evaporation. The time of flight for the ion to get detected is measured. Its corresponding data is shown in the mass spectrum.

2.5 Quartz Crystal Microbalance-Dissipation

Quartz Crystal Microbalance-Dissipation (QCMD) is a real-time, surface-sensitive technique for analyzing surface-interaction phenomena, thin-film formation and layer properties of the sample. It has dedicated sensor slots for the QCM sensors, which

detect mass changes at the sensor surface based on changes in frequency due to adsorption of mass on the sensors, whose sensitivity lies in the range of ng / cm^2. This instrument is used to detect small mass molecule surface interaction (as molecules are adsorbed and desorbed). The sensors oscillate at a 5 MHz frequency as it can optimize sensitivity, sensing depth, and the ability to perform viscoelastic modelling. Figure 2.8 represents the image of the QCM-D instrument used during the experiment[8].

Figure 2.8: Image of QCMD instrument

2.6 Electron Beam Lithography

Electron Beam Lithography (EBL) is utilized to focus a beam of electrons. It is scanned across the sample substrate covered with resist (electron sensitive material) that changes its solubility properties according to the energy deposited by the electron beam. This energy deposited is defined as the dosage of the beam. Dosage is directly proportional to the energy deposited by the electron beam. EBL schematic is very similar to that of an SEM. The electron gun is the source where the filament emits electrons either by a thermal emission source, such as a heated tungsten filament or a field emission cathode. This value is much higher in EBL than in SEM, and hence EBL has a higher etching rate of the substrate if the dosage is increased. The source value in the case of SEM is in the range of 1.2keV - 20keV. Whereas in the case of EBL, the range starts from 50keV. These electrons align with the help of a condenser lens. The condenser lens defines the resolution by defining the size of the electron beam. Subsequently, the electrons pass through the scan coils. The function of the scan coil is to control the position of the electron beam above the objective lens. The coils allow the beam to scan across the surface of the sample. These electrons pass through an objective lens which focuses the beam onto the sam-

ple [9]. The sample must be placed perfectly on the cassette and aligned perfectly in nanometer precision. It also requires a .gdsii file with the pattern/design to be etched on the sample surface. The image of the EBL used during the experiment is shown in figure 2.9

Figure 2.9: Image of EBL JEOL JBX 9300FS

2.7 Cleanroom facility

A cleanroom facility is used while fabricating structures and devices in the range of 10^{-6}m to 10^{-9}m. As the sample size decreases, the fabricating environment must have more facilities for protecting the sample. This protection decreases the probability of contaminants like particles and vibrations harming the steps of processes and the end-product performance.
The design and operation of the cleanroom are such that the introduction, generation and retention of particles are minimised. The addition of particles to the cleanroom environment is limited in many ways. By using filtering air intake, which determines the lowest achievable particle concentrations. By dressing in proper cleanroom garments such as wearing a coverall, hood, mask, gloves and boots, entering through airlocks, and thoroughly cleaning items to be taken into the cleanroom. Table 2.1 represents the simplified ISO classes which show the maximum level of particles/m^3.

Simplified ISO classes (maximum level of particles /m^3								
ISO Class	1	2	3	4	5	6	7	8
Corresponding Fed Std	-	-	1	10	100	1,000	10,000	100,000
No. of particles (>0.5 μm)	-	4	32	352	3,250	32,500	325,000	3,250,000
No. of particles (>0.1 μm)	10	100	1,000	10,000	100,000	1,000,000	-	-

Table 2.1: Simplified ISO classes (maximum level of particles /m^3)

3

Methods

3.1 Electropolishing

The metal wire samples used for electropolishing were Iron (Fe), Nickel (Ni) and Tungsten (W). The electrolyte needed for electropolishing Fe and Ni was the same. It consisted of 2 steps of electropolishing. The first step is 10% Perchloric acid (70%),20% glycerol in ethanol and the second step requires 2% perchloric acid in 2-butoxyethanol. The voltage and current parameters for electropolishing were 20 V DC and 0.150 mA. In the first step, the electrolyte is used along with inert, high-performance, fluorinated fluids-Galden. This inert fluid helps terminate the electropolishing process and is used to create a V-shape to have a uniform etching in electropolishing using 2% perchloric acid in 2-butoxyethanol[2].

The electrolyte needed for electropolishing of W wires is 5% NaOH solution and 1-5 V AC. Unlike Fe and Ni, it is a single step electropolishing process. Additional care was taken during the electropolishing process as the supply needed was AC[2]. Figure 3.1 represents the setup of the electropolishing technique.

Figure 3.1: Electropolishing setup with AC supply

The procedure for fabricating above mentioned tips is briefed. A short wire (15 mm) was taken and placed on an Aluminium holder (AH). Crocodile clips were used in order to hold the wire in the setup. A clean Platinum (Pt) strip is used as a cathode. After finishing the necessary connections to the DC supply, the electropolishing process was carried out. The stage was moved up and down on which the electrolyte was placed during the process. Only the tip submerged in the electrolyte solution gets etched to ensure uniformity in the formation of the first layer and a good V-shape. In the next stage, the specimen was subjected to electropolishing using 2% perchloric acid in a 2-butoxyethanol electrolyte[2]. It etches the submerged tips in all directions. The second step, electropolishing, is plodding due to the low concentration of the electrolyte. However, it is necessary to have a slow etching process as it has to achieve no distortions before going to the next step[10].
After the preparation of sample tips, it was observed under an optical microscope for any distortion at the apex of the sample tip. Figure 3.2, and 3.3 show the sample tip prepared using the electropolishing technique. If there were no distortions, this sample was subjected to sputtering of Gold (Au) or Chromium (Cr). It was performed to understand how field evaporation occurs between two different field evaporation rate materials when the sample tip is placed inside the field evaporation chamber in the Atom Probe.

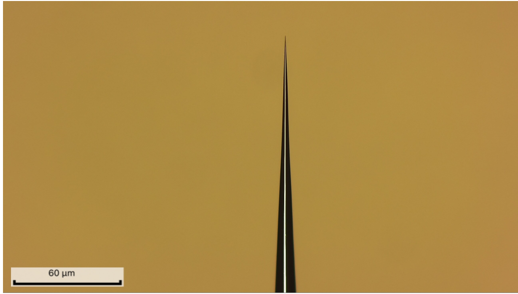

Figure 3.2: Nickel tip

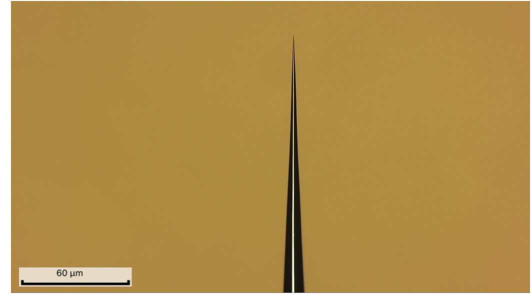

Figure 3.3: Tungsten tip

3.2 Sputter coater

The Leica sputtering instrument sputtered Au and Cr on the Ni and W tips. The instrument is vented, and the Argon valve for sputtering was opened. The required options are fed to the instrument, such as the metal to be sputtered, base vacuum, sample height, stage tilt angle, speed of rotation and thickness of sputtering. The base vacuum value, i.e. conditions where no gas is deliberately flowing into the system, was at $1.3 * 10^{-2}$ mbar, sample height was set to 15 mm, stage tilt angle was set to -30°and was set to rotate at speed number 5 (varies from 1-5).
The instrument had an inbuilt option for using the thickness required to be sputtered in the manual or automatic mode. The instrument uses a Quartz crystal to measure the thickness sputtered on the sample tip in the automatic mode. The current and time parameters must be fed in manual mode as the instrument does not use the quartz crystal measurements for the same. In addition, the sputtering rate in the manual mode is three times slower than in the automatic mode. The manual

mode sputter-coated the sample for different time ranges. The correlation between the shown thickness value to the actual sputtered thickness, in the manual mode, was plotted in excel, and the thickness-time curve is shown in figure 3.4. This curve helped choose the time value to be fed to the instrument to achieve the corresponding thickness.

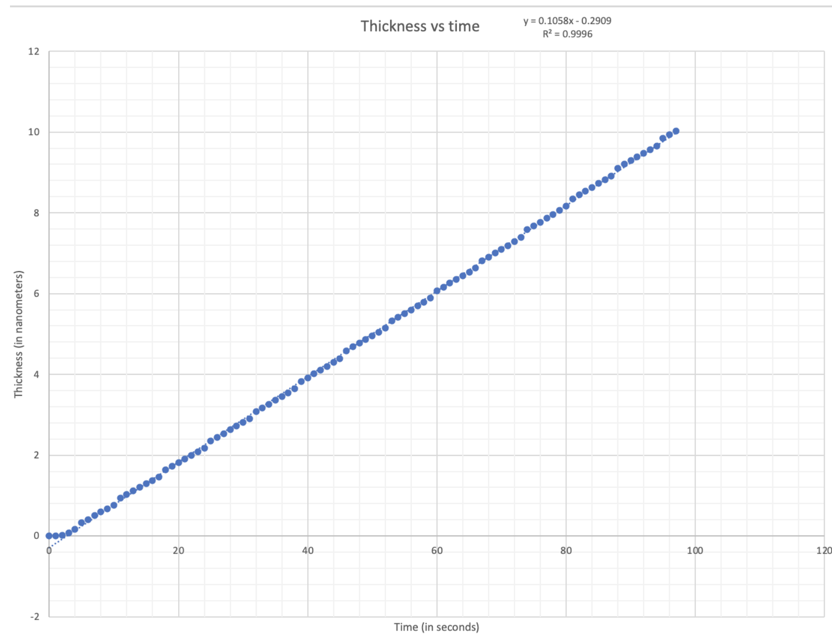

Figure 3.4: Time versus thickness plot

3.3 Fabrication of Silica chip

This step was performed in the cleanroom facility at the MC2 department in Chalmers. Before fabricating the silica tips, the silicon chip must undergo a few cleaning procedures and spin coating of silica on the silicon chip.
The silicon chip was cleaned using the Piranha solution. It is a mixture of Water, Ammonia and Peroxide in a 5:1:1 ratio. The cleaning was carried out at 80°C to prevent the boiling of water during cleaning. The Si chips were placed in a UV ozone cleaner for 30 minutes to remove any impurities on the surface. It was rinsed thoroughly in milli-q water and dried using nitrogen gas. Once the surface was cleaned using the above method, SiO_2 was spin-coated on its surface. The thickness of spin-coated SiO_2 was approximately 200 nm. The silica on silicon chips was placed in a hot oven at 37°C temperature to dry the silica film. Sodium silicate solution was prepared by mixing the stock solution in milli-q water in 1:3 ratio. It was later run through an ion exchange column to adjust the pH. Solid silica was prepared using the alkoxide tetraethyl orthosilicate (TEOS) and sodium silicate (water glass) as silica precursor. Silicon alkoxides spontaneously hydrolyze when in contact with water. It condenses to form an amorphous polymer network of silicon and oxygen. The reaction is catalyzed both by acidic and basic conditions and is foremost dependent on the organic moieties of the alkoxide, pH, concentration, and temperature. The

formed solid's gelling time and physical properties such as porosity can be controlled by varying these parameters.
For fabricating the design on the silica on silicon chip, Electron Beam Lithography (EBL) was used. The input for the design in the EBL must be in the .gdsii file. The circle array, which was exported in a .gdsii file, was designed using K Layout software. The image of the design is shown in figure 3.5

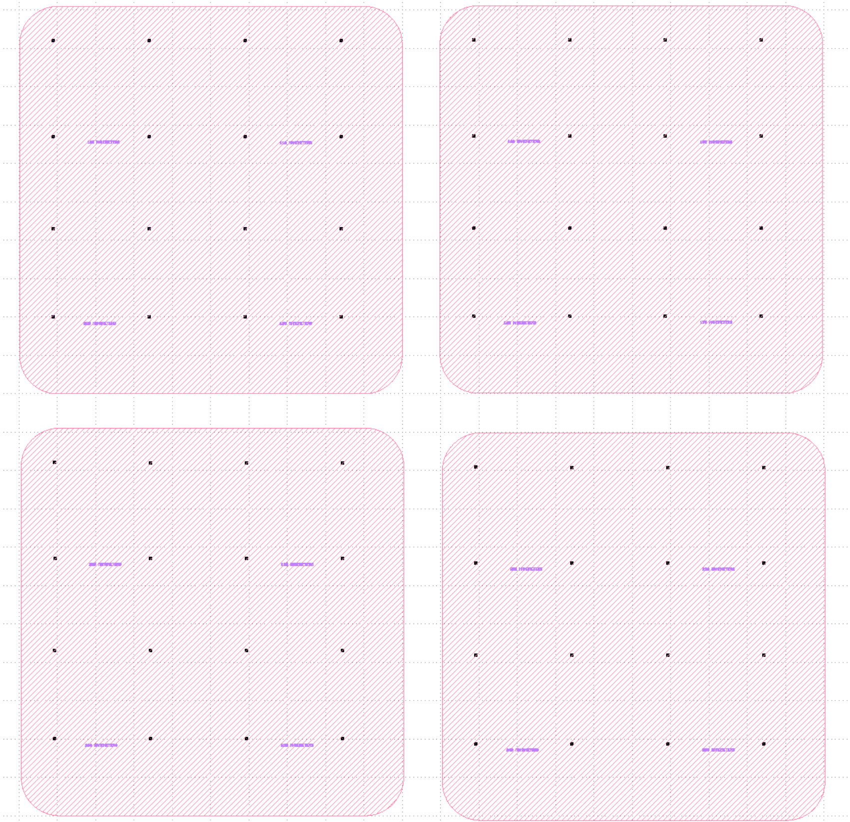

Figure 3.5: Design of pattern in K Layout

The silica on silicon chip has to undergo a few more procedures, including the spin coating of negative photoresist, MAN-2403 at 3krpm for 60 seconds which coated 300 nm on the surface. The chip was cleaned using Reactive Ion Etching/ Oxygen Plasma for 1 minute at 100W[11]. The chip was subjected to baking on a hot plate at 130°C for 2 minutes. The next step involved spin coating of Ti Prime at 3000krpm[12]. It is a primer used to improve the resist adhesion on the surface. It was also used because Ti prime can be etched by Hydrofluoric acid (HF)[13]. The sample was soft baked on a hot plate at 90°C for 2 minutes. The next step involved exposure in EBL, where the design was loaded as a .gdsii file. The next step involved the development of the sample in MF24A for 60 seconds and rinsing thoroughly in water[12]. The image of the silica on silicon chip before the HF and KOH etching is shown in figure 3.6

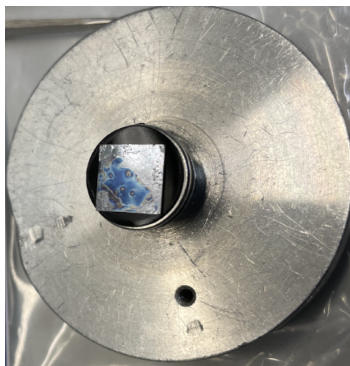

Figure 3.6: Image of silica on silicon chip after EBL array design

3.3.1 Hydrofluoric acid etching of silica

Hydrofluoric acid (HF) etching of silica was carried out in the cleanroom. A thorough risk assessment was carried out, and protection gears such as chemical gloves, HF protection gloves, chemical apron and visor were worn. HF protection gel was made sure to be within hand reach. A test sample was used to determine the etching time required for the silica layer. Since the different dosage of the array was patterned, the time required for etching dosage-450 was determined. However, due to the non-uniform layer of silica on the surface, uneven etching of silica was observed. Hence, Buffered oxide etch (BOE) was used as it has a uniform etch rate of 80 nm per minute. BOE is prepared by mixing 6:1 volume ratio of 40% NH_4F in water to 49% HF in water. The silica on silicon chip was etched in BOE for 1 minute, even though the thickness of the silica layer was 200 nm.

3.3.2 Potassium Hydroxide etching of silicon

Potassium Hydroxide (KOH) etching of Si was also carried out in a heated water bath in the cleanroom. The concentration of KOH used was 35%. The temperature maintained in the water bath was 85 °C in order to maintain 80 °C in the KOH solution. The etching rate of Si by KOH was found to be 1.25 micrometres per minute and 1.875 micrometres at 80 °C for <100> Si and <110> Si orientation, respectively. KOH also etches the silica at a meagre rate of 6.6 nm per minute, which further etches the silica layer after HF etching [14].

3.4 QCMD

Quartz Crystal Microbalance-Dissipation (QCMD) was used to analyse the binding property of the protein on different surfaces such as Gold, Chromium and Gold Nanoparticles (GNP) on a chromium sensor. Beneath the sensor is a thin quartz crystal disk with electrodes deposited on each side. This oscillating unit, via applied voltage, oscillates at the resonance frequency. The instrument performs the measurements based on the quartz crystal's oscillating frequency and the dissipation frequency when mass is detected on the sensors[8]. The QCMD sensors were coated with the materials mentioned above.

The first step involved cleaning the sensors. The sensors were cleaned using the Piranha solution. It is a mixture of Water, Ammonia and Peroxide in a 5:1:1 ratio. The cleaning was carried out at 80°C. It was to ensure the water did not escape from the mixture. The sensors were subjected to ultrasonication while immersed in a beaker with 2% sodium dodecyl sulfate (SDS) solution for 20 minutes. It was rinsed thoroughly in milli q water and again subjected to ultrasonication while immersed in milli q water for 20 minutes. The sensors were rinsed thoroughly and dried using nitrogen gas.
The QCMD instrument is connected to a pump which can maintain a constant flow rate at a very slow rate. The flow rate at which the experiments were conducted was 90 microlitres per minute. Once the clean sensors were placed in their respective locations, the inlet and outlet for liquid were connected accordingly. Firstly, water was made to flow through the sensors. The changes in frequency and the time of inlet of solution were noted down when no further changes were ensured. Next, Phosphate-buffered saline (PBS) was introduced at the same flow rate, and the changes were observed. Succeeding this step is the inlet of protein solution diluted in PBS buffer. The changes in frequency were observed, and the inlet time was noted. This point was the end of the experiment, but the cleaning of the tubes and sensors was pending. The cleaning protocol was followed, and the frequency changes were observed to go back to the initial state.

3.5 Atom Probe Tomography

The Atom Probe Tomography (APT) tips were placed on a coupon, which was placed in the loading chamber. The next step involved the coupon transfer into the APT chamber for analysis. There are two modes for APT analysis: Pulsed voltage and laser voltage[15]. The sample has to be aligned to the detector. Once the experiment was ready to be commenced, the voltage pulse was increased gradually—the sample experiences high field evaporation. Every material had a field curve when its voltage and temperature were plotted[2]. Below the field curve, field evaporation is unlikely to occur. Upon varying the temperature or voltage, field evaporation can occur. The voltage pulse was increased until no more field evaporation took place in the APT chamber. The temperature parameter set during the experiment was 50 K. After the APT analysis, the data acquired was used to perform the sample's image reconstruction.
There were seven instruction steps for carrying out the image reconstruction of sample tips. The software had to be calibrated to determine the radius of the tip in the ROI. It was carried out with the help of an SEM image of the analysed sample. The results analysed are discussed in the results section.

4 Results

4.1 Electropolishing and sputter coating

After analyzing the SEM images of the electropolished tips, the operating procedure was improved to consistently get sharper tips during electropolishing[2]. These electropolished tips were sputter-coated with different thicknesses (in manual mode) to find a correlation between time and thickness of sputter coating. The parameters for which set thickness and measured thickness were equal at $1.3 * 10^{-3}$ mbar pre sputter vacuum—this analysis aided in predicting how the APT reconstruction of the sample would appear.
Due to external factors such as mishandling of sample, contaminants, and high air pressure change, to name a few, the sample was distorted slightly[10]. It affected the APT analysis and the reconstruction of image. It will be discussed in the later section of the report. Figure 3.4 was used as the reference for analyzing the Region of Interest (ROI), which will be discussed in the later section of this report.

4.2 Wet etching of silica on silicon chip

The SEM images of the etched silica on silicon chip are shown in figure below. Due to appearance of unknown entities on the surface, some images are shown in Appendix A.

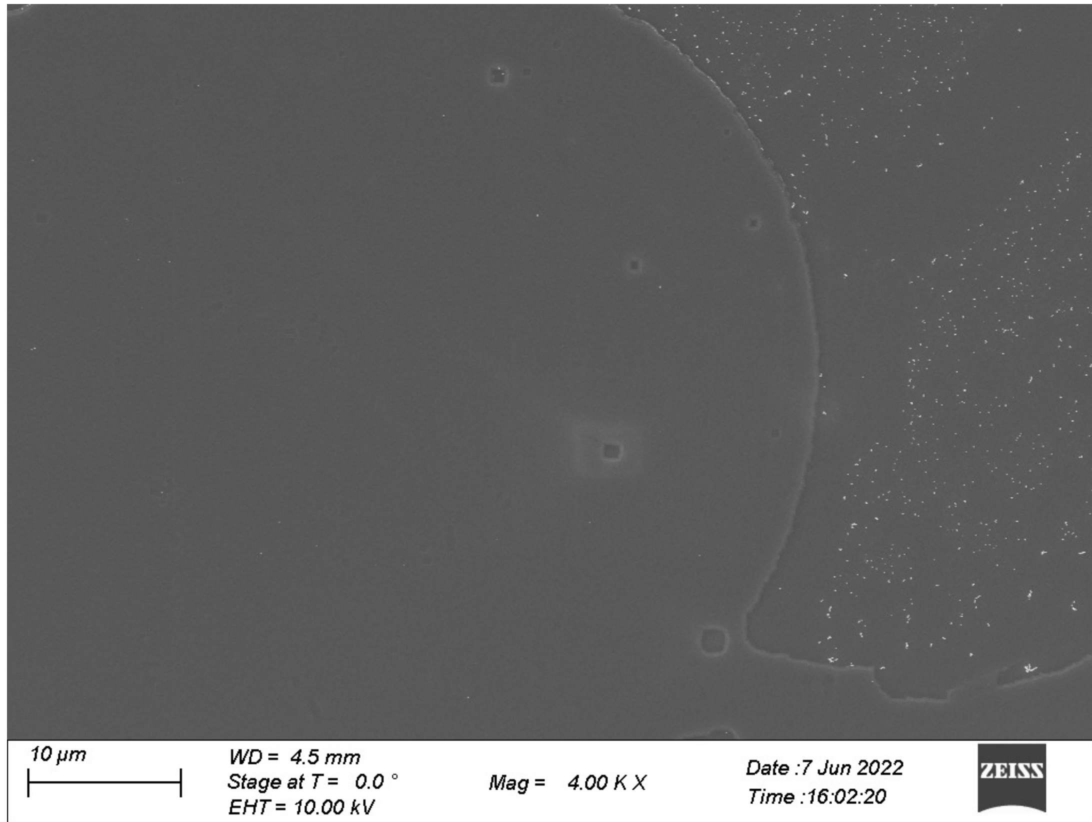

Figure 4.1: Image of surface after HF and KOH etching

4.3 Imaging of samples

The SEM images of electropolished tips and its corresponding gold sputter-coated tips are shown in figure 4.7,4.8, 4.9, 4.10, 4.11 and 4.12. The images captured aided in analysing the thickness of the material sputter coated. Using the data obtained from Figure 3.4, the set thickness value was set to its corresponding time value. For example, in figure 4.7 and 4.8, the sputter coater had different parameters. The base vacuum pressure was maintained at $1 * 10^{-3}$ mbar, and the current was set at 60 mA. The required sputter coat thickness was 35 nm. From figure 3.4, it was inferred that 96 seconds sputter-coated 10 nm thick film on the surface. Hence for 35 nm, 336 seconds was set as the time value. However, in figure 4.11 and 4.12 the sputter coater had different parameters. The base vacuum pressure was maintained at $1 * 10^{-2}$ mbar, and the current was set at 30 mA. The required sputter coat thickness was 35 nm. Nevertheless, upon measuring the sputtered thickness, the value was found to be 100 nm of gold-sputtered near the apex of the W tip.
SEM images of Si chip after EBL lithography are shown in Appendix A. It was captured to judge the appropriate dosage, which has to be set for etching on the actual Si Chip sample[16]. Different dosage etches different depth circles, affecting HF and KOH etching time. Thus, it was essential to identify the appropriate dosage value for etching the Si chip sample. However, not all doses were completely patterned with the non-uniform spin coating of SiO_2 on the Si chip. The patterned images where the circles of different diameters were imaged were where SiO_2 was present.

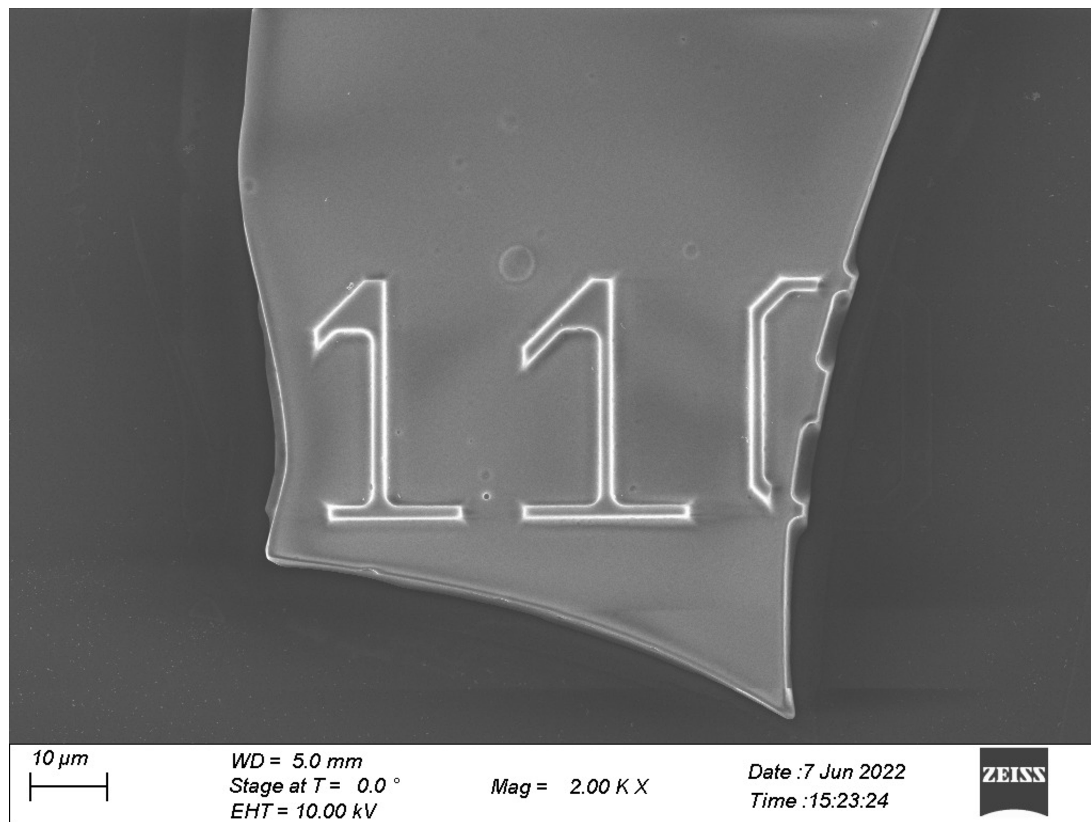

Figure 4.2: Image of 110 nanometers etched on the surface

4.4 Atom Probe Tomography

The software used for the reconstruction of the APT sample tips was IVAS Standard 3.6.14. The samples considered for analysis were Ni tip, Au sputtered Ni tip (Ni-Au), W tip, and Cr sputtered Nickel tip (Ni-Cr).Due to distortion at the apex of the Ni-Cr tips, it was challenging to align it near the detector. Subsequently, the major problem with the Cr-coated specimen was that the Cr layer was oxidized, making it very difficult to run in voltage mode. In addition, due to the large size of W tips(225 nm), it was difficult to analyze in the APT, and the tip underwent a fracture during analysis. It was due to the large size at the W tip, high field was required to achieve field evaporation. This high potential might have caused stress at the apex of the tip, causing it to damage and fracture [2].
A smaller section of the reconstructed image is analyzed. Figure 4.13 shows the spatial distribution of the ROI of the Ni-Au tip.. It means that each count which was detected is an atom or molecule of several atoms. Figure 4.15 shows the image of the 2D contour of the oxide layer formed in the ROI. The cross sectional image of the Ni-AU tip is shown in figure 4.16. The mass spectrum data obtained during the APT analysis was plotted on a logarithmic scale. The raw data received from APT was plotted on excel without a logarithmic scale to identify other elements detected with significant counts. The non-logarithmic scale is rarely used as it gives very little information. However, since the total ions detected were a few hundred thousand, the less significant count, compared to Ni atoms, was identified. Figure

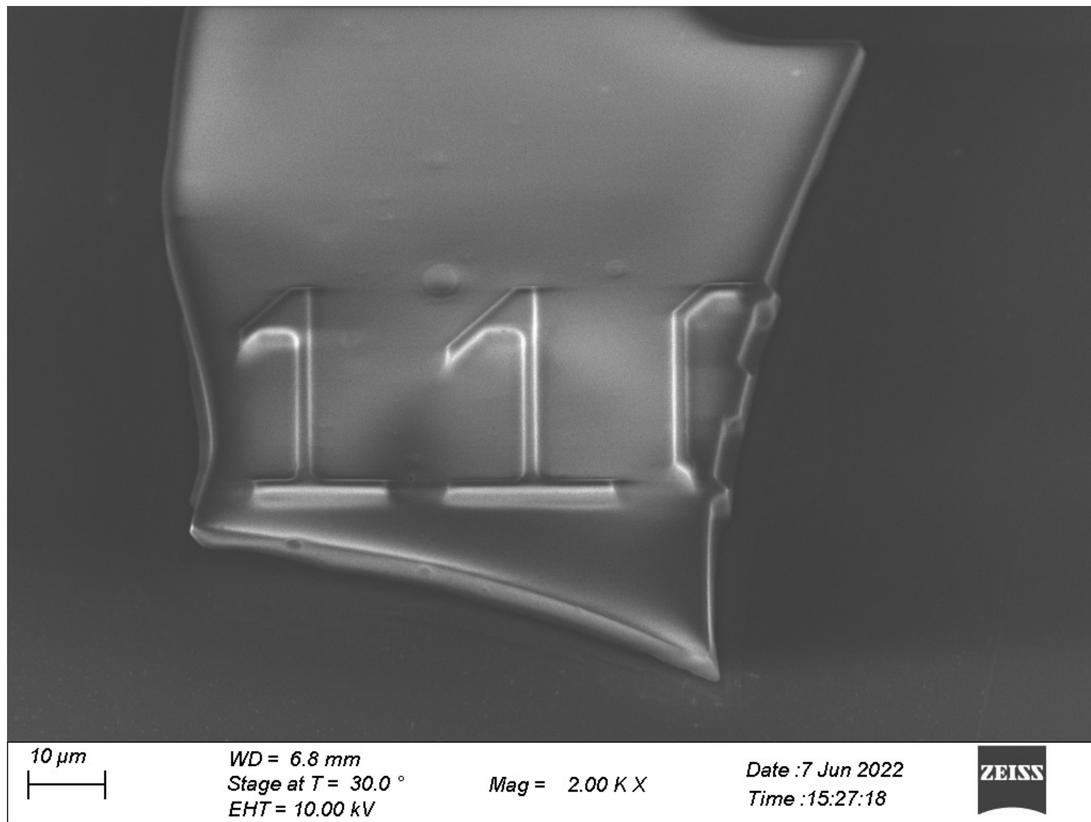

Figure 4.3: Image of 110 nanometers etched on the surface at 30 °

4.17 and 4.18 represent the mass spectrum with and without the logarithmic scale, respectively. The elements identified on the mass spectrum along with the possibility of its detection are Hydrogen, Carbon, Nitrogen, Oxygen, Nickel, oxides of Nickel, Chlorine and Aluminium. During the image reconstruction of tips, it was observed that field evaporation took place only on one side of the tip. It was believed to occur due to the distortion of the tip. In addition, the ROI of the Ni-Au tip does not show any gold atoms. It can also be due to the possibility of out-of-field evaporation due to the small detector size. In addition, the distorted tip and imperfect alignment decreased the probability of detecting the gold atoms. The observed area detected in the APT of the Ni-Au tip is different from the actual area that was supposed to be detected [2]. The Au atoms might have achieved field evaporation. However, it did not get detected due to the involvement of the field area of the detector.

A smaller section of the reconstructed image is analyzed. Figure 4.13 shows the spatial distribution of the ROI of the Ni-Au tip. Figure 4.14 represents the legend for the detected ions in the mass spectrum during image reconstruction. The legend can be used as a reference for identification of the detected ions which are correspondingly colour coded. It means that each count which was detected is an atom.image Figure 4.15 shows the image of the 2D contour of the oxide layer formed in the ROI. The cross sectional image of the Ni-AU tip is shown in figure 4.16. Upon analysing the cross-sectional image, comparison of detected atoms versus actual atom present was carried out[2].The mass spectrum data obtained during the APT analysis was plotted on a logarithmic scale. The raw data received from APT was plotted on

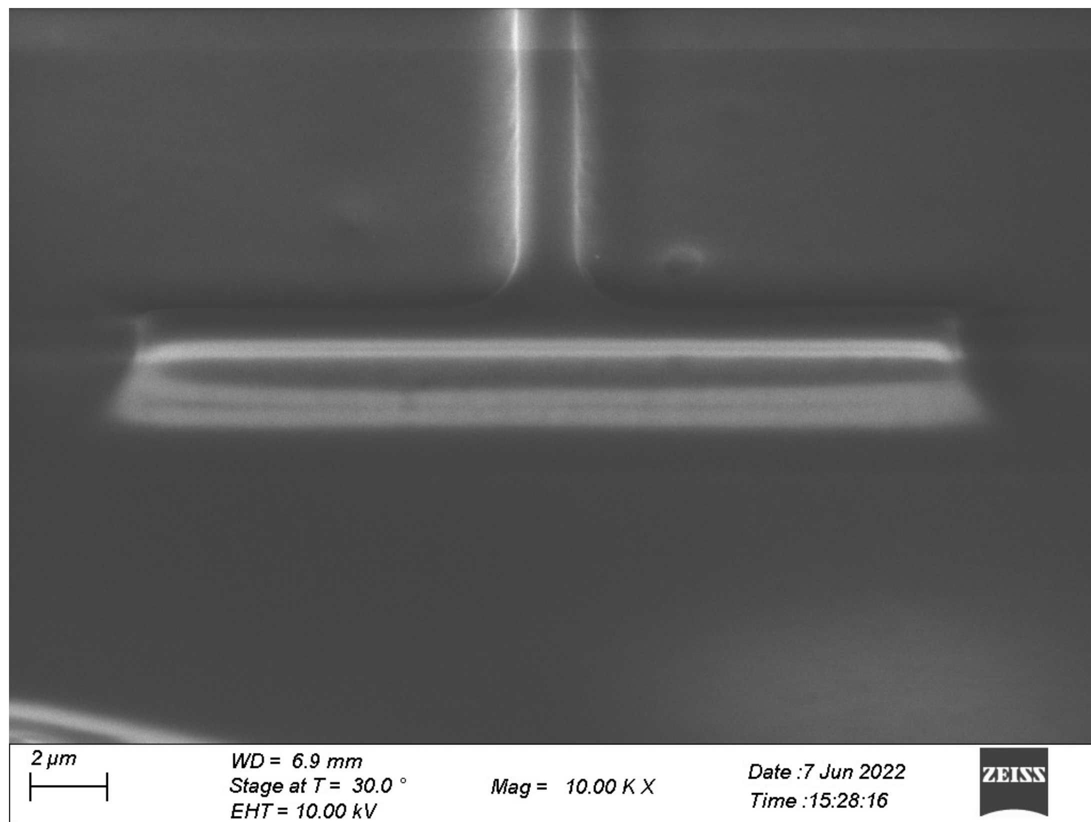

Figure 4.4: Image of 110 nanometers etched on surface at 30 °and 10kX zoom

excel without a logarithmic scale to identify other elements detected with significant counts. The non-logarithmic scale is rarely used as it gives very little information. However, since the total ions detected were a few hundred thousand, the less significant count, compared to Ni atoms, was identified. Figure 4.17 and 4.18 represent the mass spectrum with and without the logarithmic scale, respectively. The elements identified on the mass spectrum along with the possibility of its detection are Hydrogen, Carbon, Nitrogen, Oxygen, Nickel, oxides of Nickel, Chlorine and Aluminium. During the image reconstruction of tips, it was observed that field evaporation took place only on one side of the tip. It was believed to occur due to the distortion of the tip. The side with less detected ions is the side where oxides were present. The oxide phase can have a higher field, which leads to less evaporation at the operated settings. In addition, the ROI of the Ni-Au tip does not show any gold atoms. It can also be due to the possibility of out-of-field evaporation due to the small detector size. Subsequently, the distorted tip and imperfect alignment decreased the probability of detecting the gold atoms. The observed area detected in the APT of the Ni-Au tip is different from the actual area that was supposed to be detected [2]. The Au atoms might have achieved field evaporation. However, it did not get detected due to the involvement of the field area of the detector.

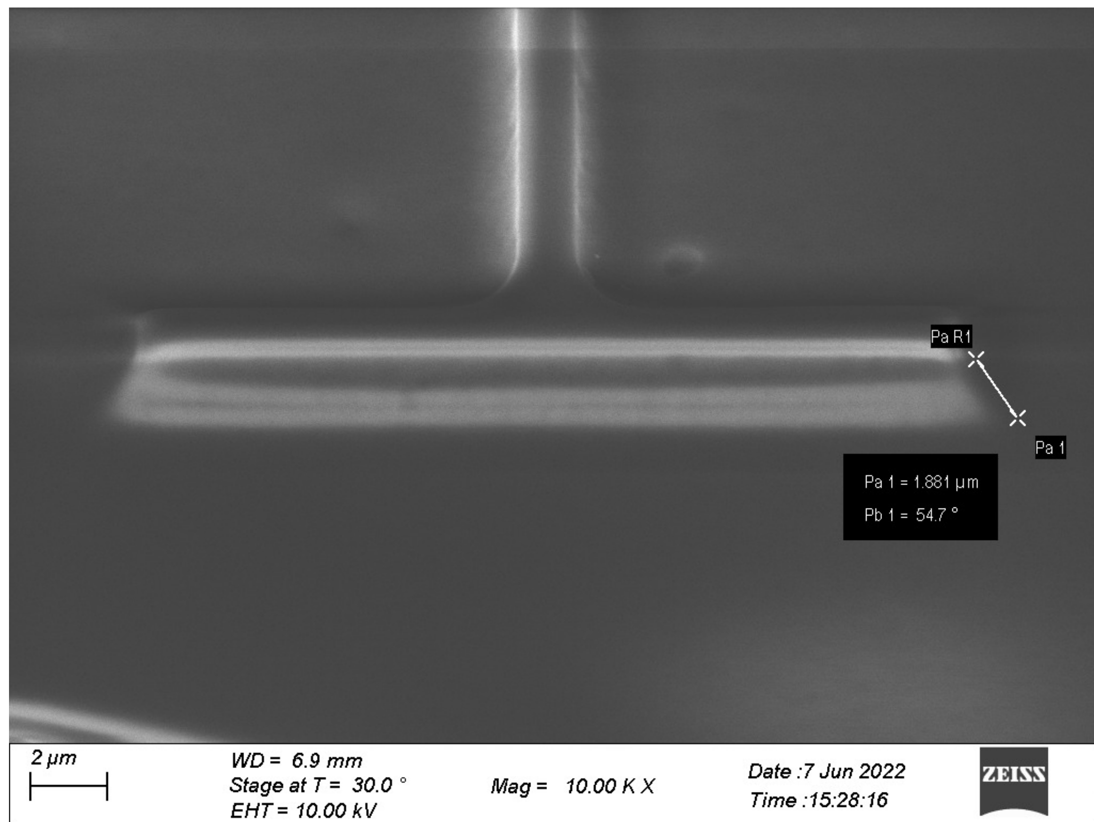

Figure 4.5: Image of the angle formed of 110 nanometers etched on the surface at 30 °

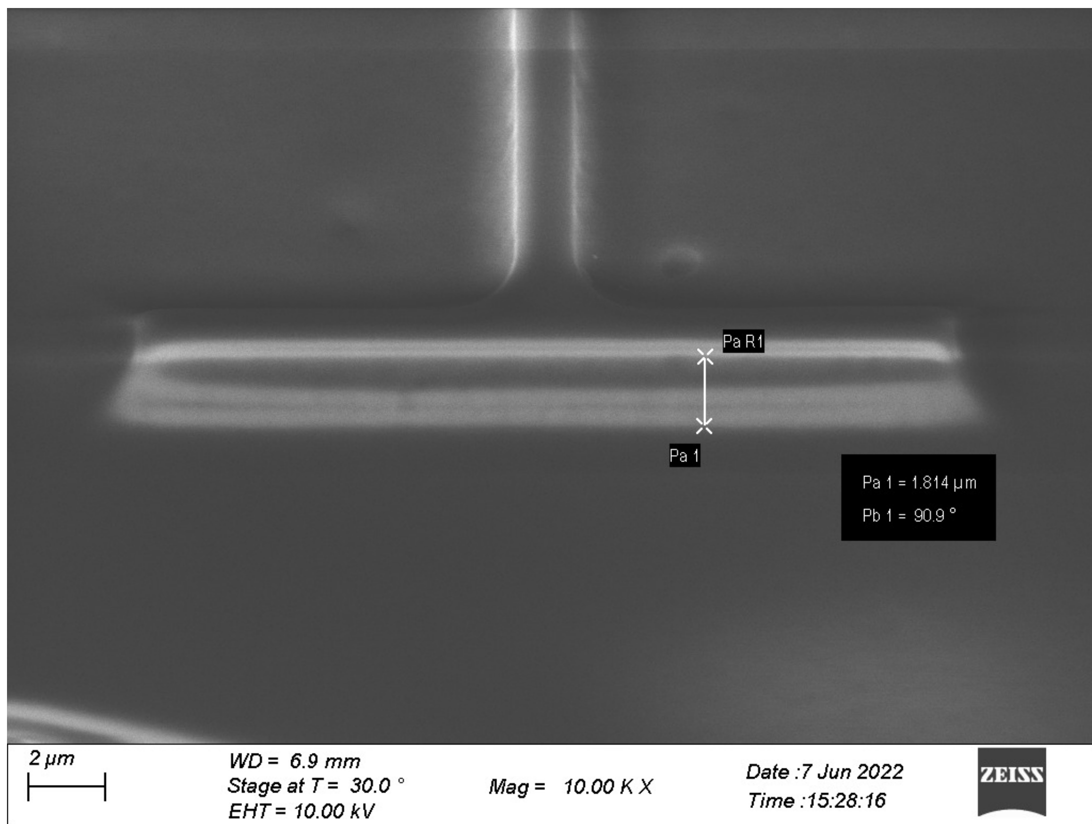

Figure 4.6: Image of etched height of 110 nanometers etched on the surface at 30°

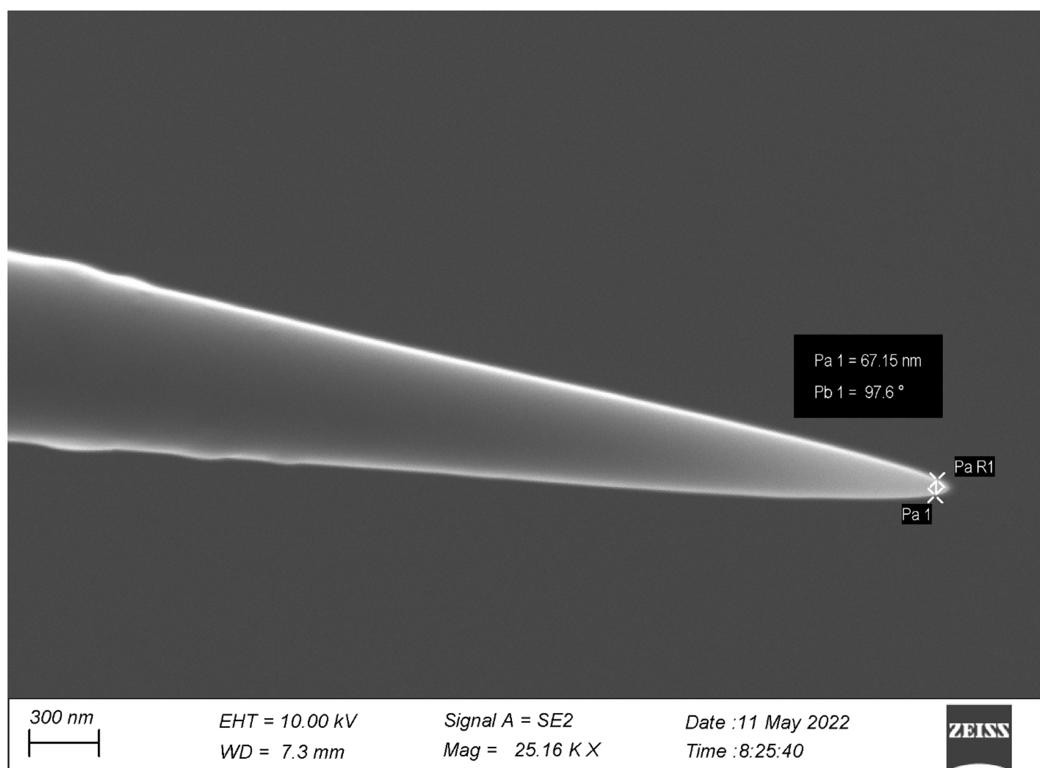

Figure 4.7: Nickel tip

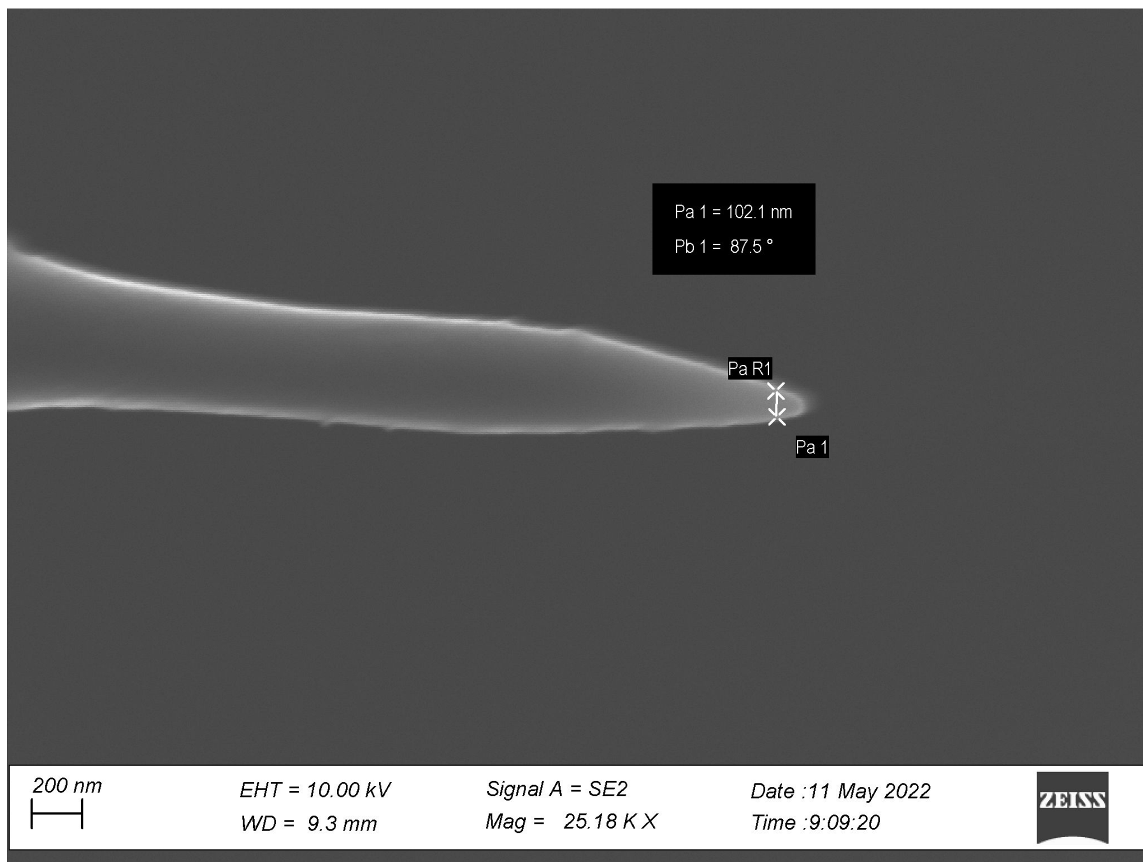

Figure 4.8: Gold sputtered Nickel tip

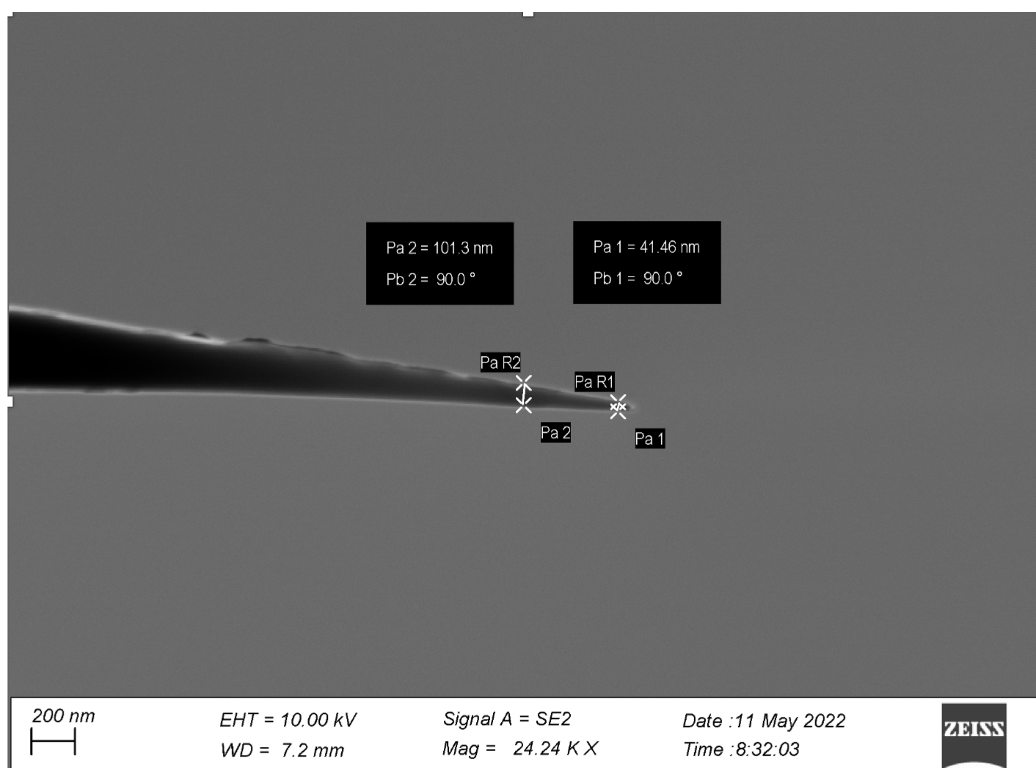

Figure 4.9: Nickel tip

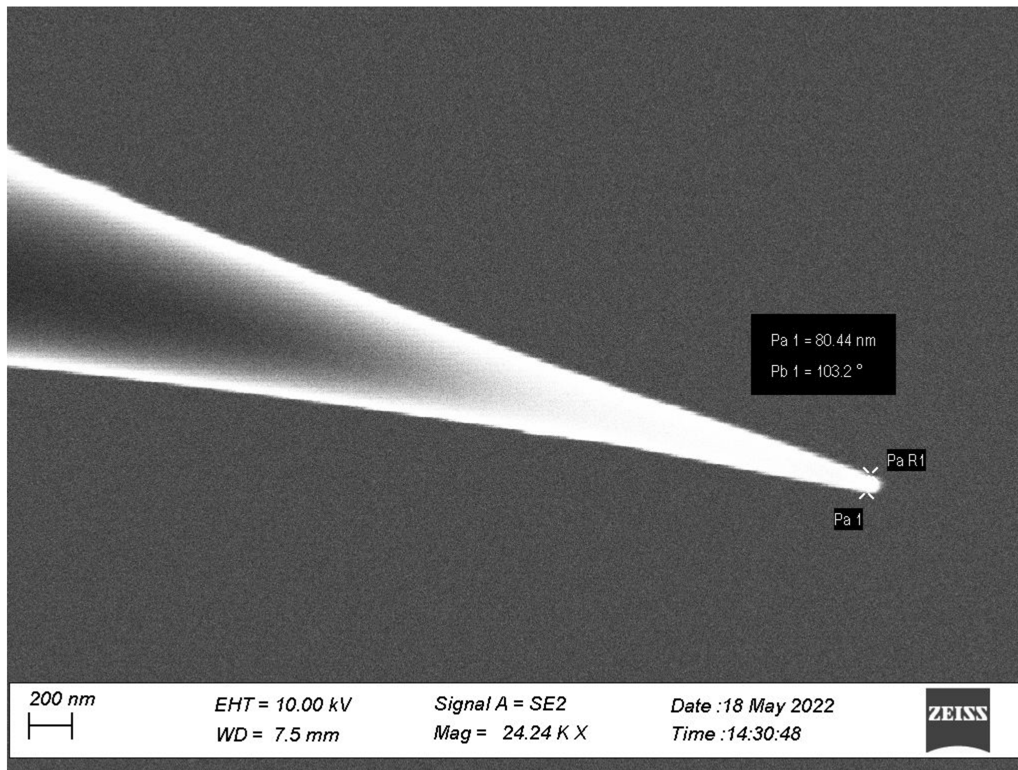

Figure 4.10: Gold sputtered Nickel tip

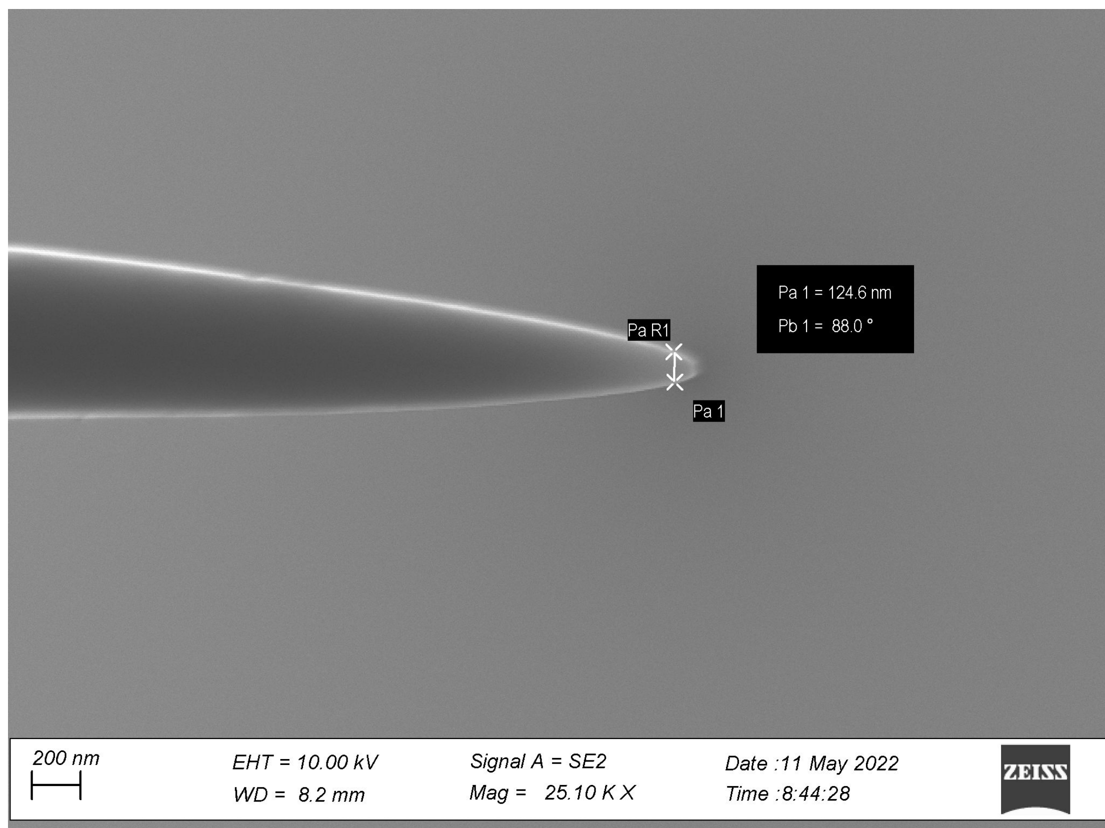

Figure 4.11: Tungsten tip

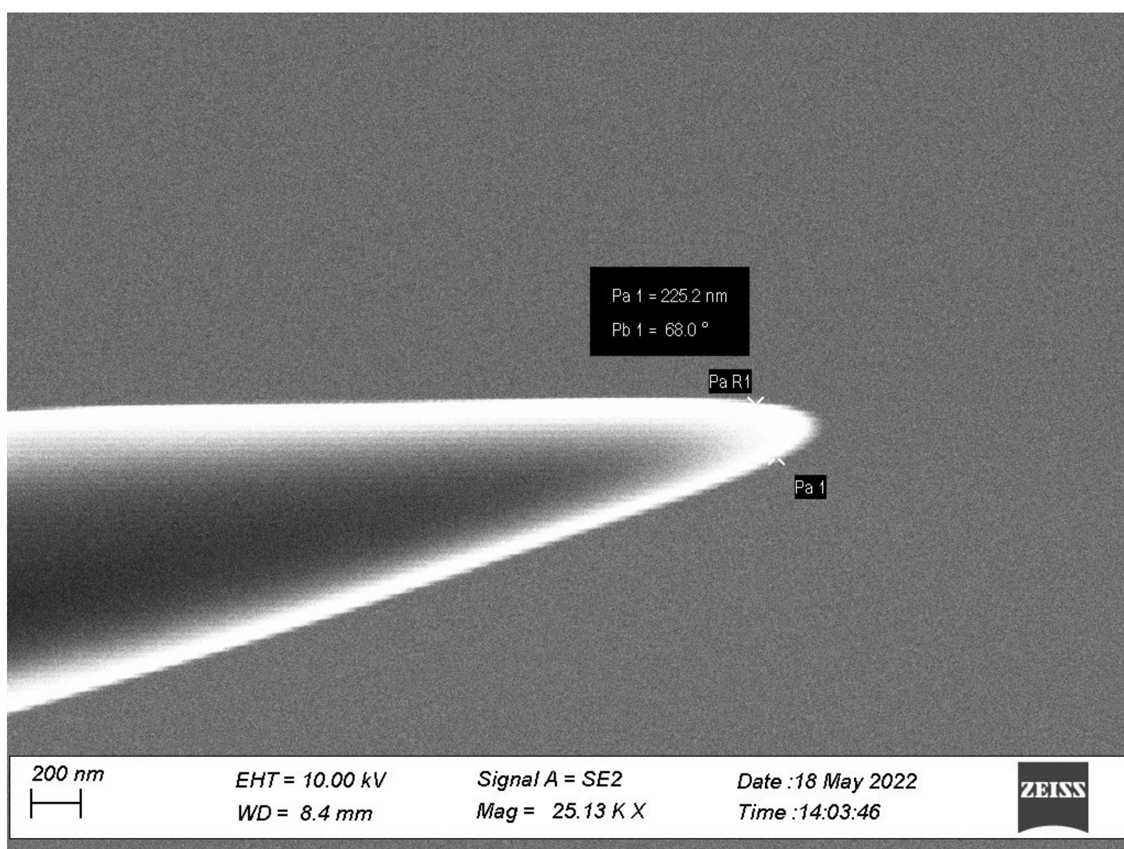

Figure 4.12: Gold sputtered Tungsten tip

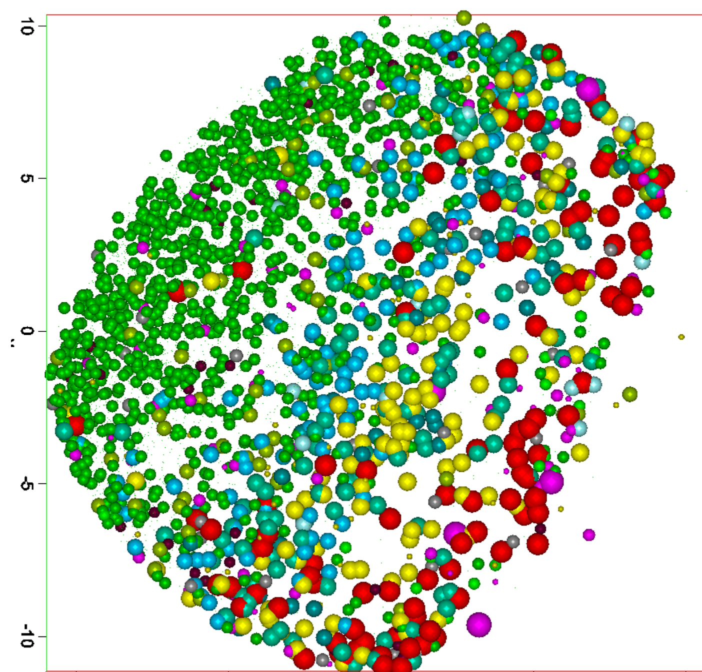

Figure 4.13: Spatial distribution in ROI of Ni-Au tip

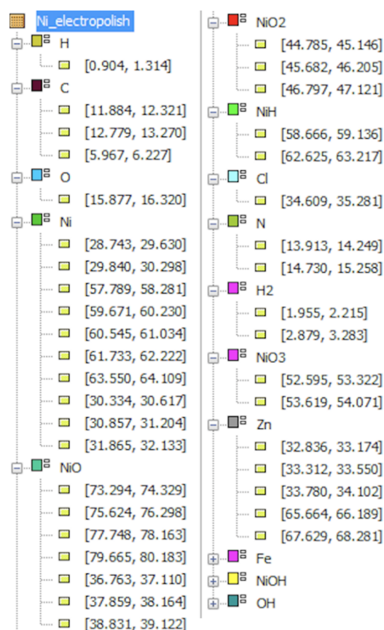

Figure 4.14: Legend representing the detected ions in the mass spectrum during image reconstruction

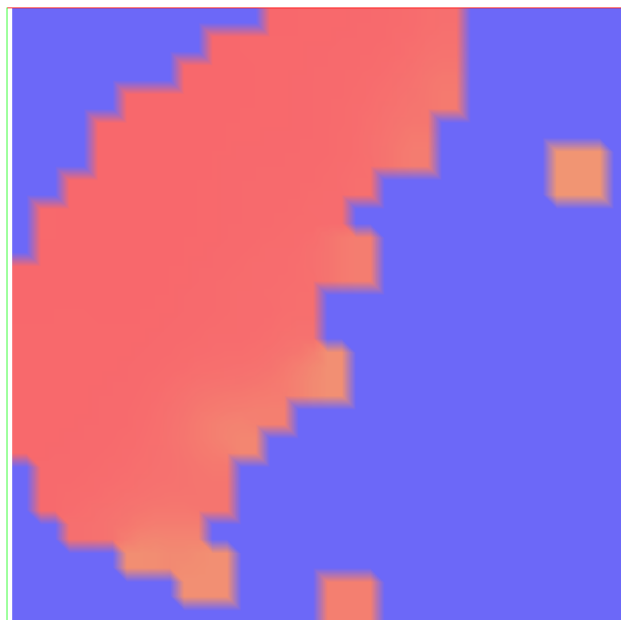

Figure 4.15: 2D contour of the oxide layer in Ni-Au tip ROI

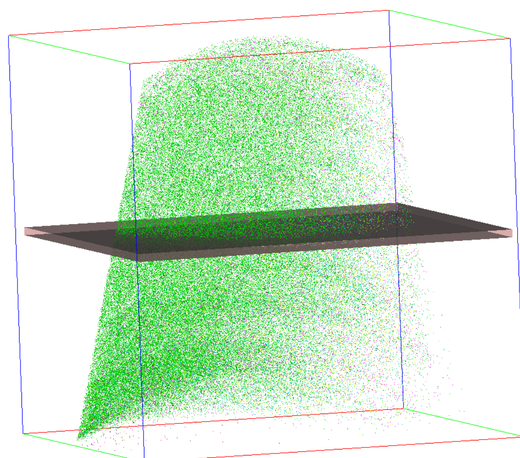

Figure 4.16: Cross sectional image of Ni Au tip

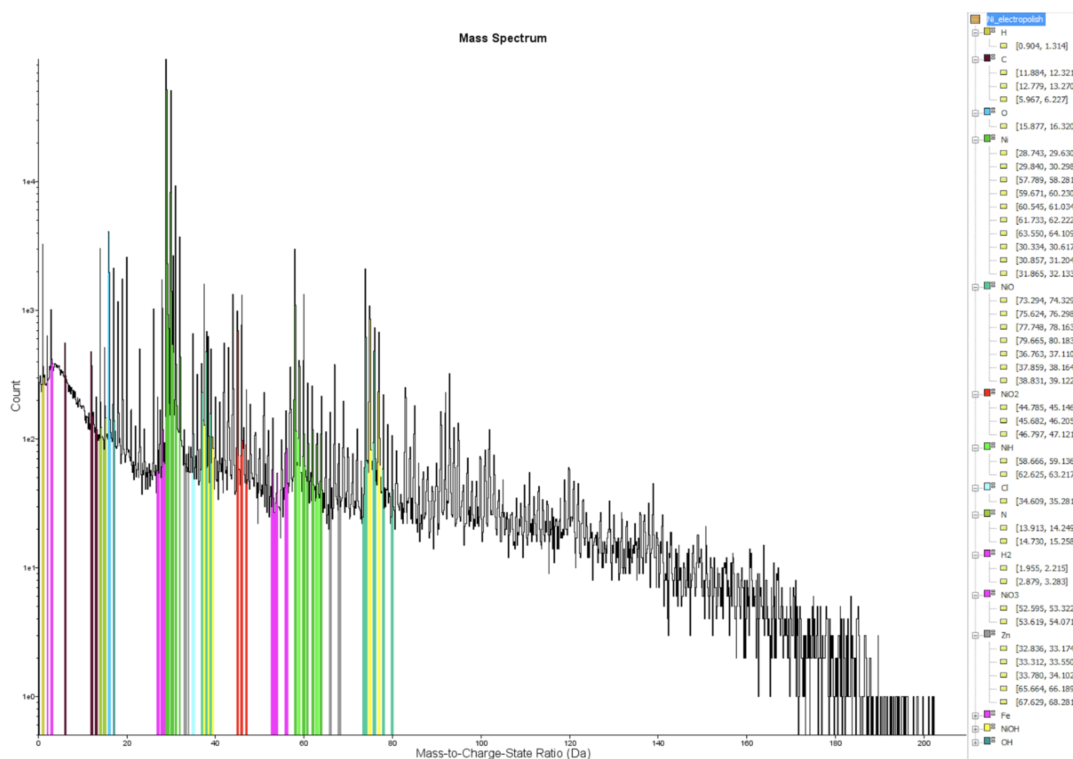

Figure 4.17: Mass spectrum of Ni-Au tip on logarithmic scale

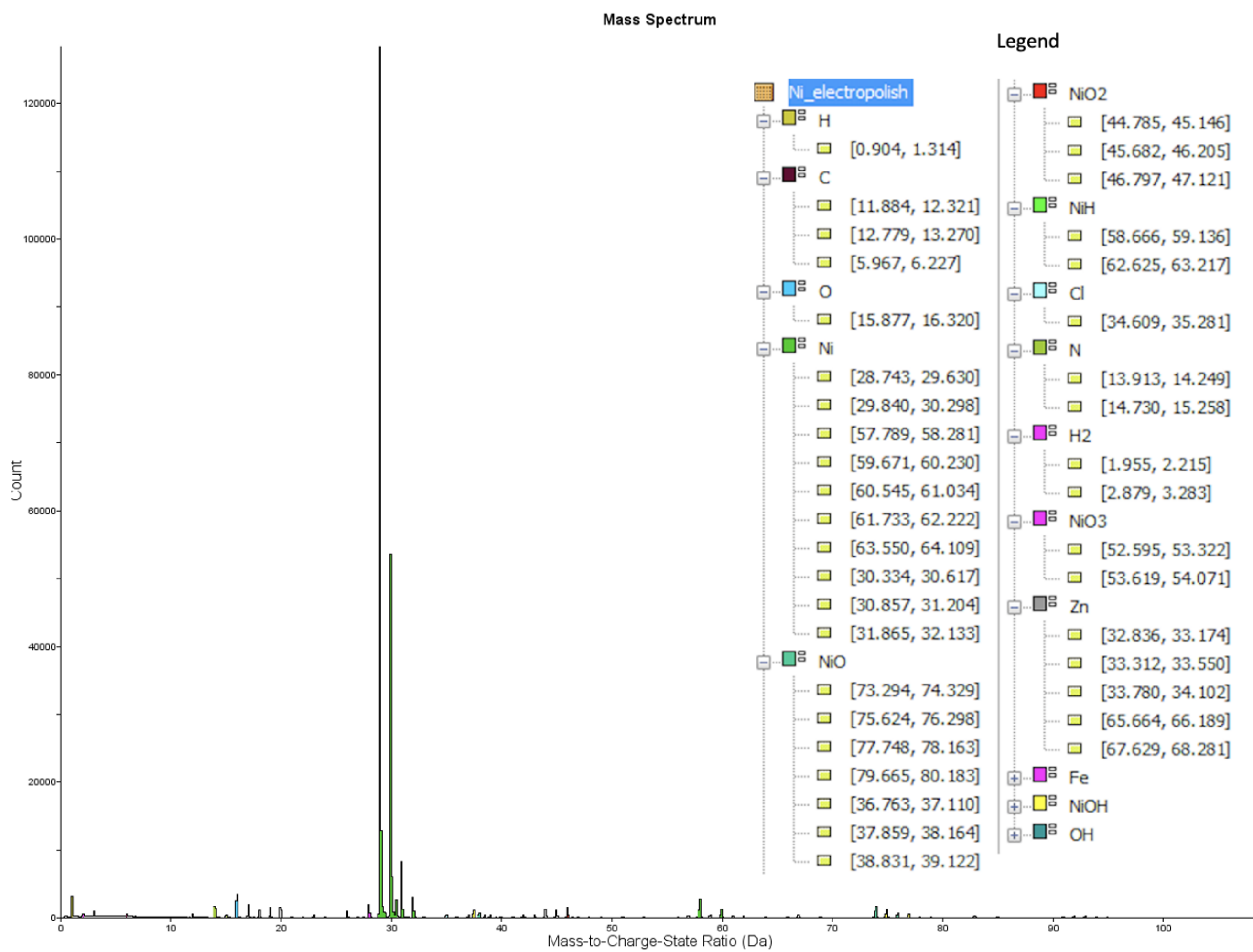

Figure 4.18: Mass spectrum of Ni-Au tip

5 Conclusion

The detection of Hydrogen, Carbon, Nitrogen and Oxygen was likely due to the atmospheric exposure of the tip. The detection of Nickel is self-explanatory. However, the detection of oxides of Nickel was almost certainly due to the atmospheric exposure or oxidation of Nickel during sputter coating [17]. The detection of Chlorine atoms was likely due to the usage of 10% and 2% Perchloric acid as electrolytes during electropolishing. The detection of Aluminium was most likely due to the presence of Al on the Ni tip surface.. The detection of Hydrogen, Carbon, Nitrogen and other elements maybe because of residues on the surface during transfer of the sample. The low detection count of H,C N, Cl and Al had low count because, in the bulk composition Ni is dominating.

The standard operating procedures for electropolishing were improved to produce identical tips. It helped in developing the sputter coating thickness vs time plot. Subsequently, the appropriate sputter coating parameters were set and saved in the instrument. Due to external factors such as mishandling of sample, contaminants, and high air pressure change, to name a few, the sample was distorted slightly[2].

It affected the APT analysis and the image reconstruction of ROI. The atom probe instrument has an out-of-field view within which no detection occurs. The field view of the instrument is about 30°. When the tip is distorted, the out-of-field view increases[2]. It loses more data in during detection. The out-of-field view might be the reason for not detecting gold atoms during the APT analysis. The oxide can, as discussed, be due to the sputter coating, meaning that that region is close to the gold interface. Gold also has a higher field than Ni, which can explain the lack of detected gold.

The QCMD experiment involved the study of the binding of the thiol protein on the surface of gold, chromium and GNP on chromium surface. However, due to fault in piping, the correct data was not achieved and hence not published in this report.

After the patterning of the design in the EBL, the Si chips had the exact dimensions as the design due to selecting the accurate dosage (dosage 450) during the etching process[16].

After the etching of silica on silicon chip with HF and KOH, the 110 nanometers text was observed in the SEM. After tilting the SEM stage to 30 °, the height of the etched surface was observed and measured. The angle formed due to the anisotropic

etching was also observed to be 54.7°, and it agrees with the reference paper [14]. Upon magnifying to 60kX, the patterned circle was observed near the 110 nm text. However, upon measuring the diameter, it was confirmed that the circle was not of the 110 nm diameter as its diameter was measured to be 400nm. Appendix A also represents other images, which were not identified yet interesting to see, which were observed on the silica on silicon surface.

5.1 Future Work

The scope for performing APT analysis on sputter-coated metal tips without any distortions can be studied. The formation of the oxide layer during the sputter coating and means of reducing the oxidation on the surface can be investigated.

Fabrication of silica on silicon tips using wet etching to achieve the desired tips for APT analysis can be studied in detail. Techniques to embed the proteins to be analysed can be studied to overcome obstacles such as soft baking of chip during fabrication and the KOH wet etching, performed at 80°C.

Comparison of sputter-coating different materials on silica on silicon tips and the APT analysis of the tips can be examined.

Bibliography

[1] Yuxiu Gong et al. "Visualizing hazardous solids with cryogenic electron microscopy (Cryo-EM)". In: *Journal of Hazardous Materials* 436 (Aug. 2022), p. 129192. ISSN: 0304-3894. DOI: 10.1016/J.JHAZMAT.2022.129192.

[2] M. K. Miller. *Atom Probe Tomography.* Springer US, 2000. DOI: 10.1007/978-1-4615-4281-0.

[3] D. K. Schreiber et al. "A method for site-specific and cryogenic specimen fabrication of liquid/solid interfaces for atom probe tomography". In: *Ultramicroscopy* 194 (Nov. 2018), pp. 89–99. ISSN: 18792723. DOI: 10.1016/j.ultramic.2018.07.010.

[4] Amir Pourabed et al. "High throughput acoustic microfluidic mixer controls self-assembly of protein nanoparticles with tuneable sizes". In: *Journal of Colloid and Interface Science* 585 (Mar. 2021), pp. 229–236. ISSN: 0021-9797. DOI: 10.1016/J.JCIS.2020.11.070.

[5] Rémi G. Tilkin et al. "Protein encapsulation in mesoporous silica: Influence of the mesostructured and pore wall properties". In: *Colloids and Surfaces A: Physicochemical and Engineering Aspects* 642 (June 2022), p. 128629. ISSN: 0927-7757. DOI: 10.1016/J.COLSURFA.2022.128629.

[6] "Chapter 2 Physics of sputtering". In: *Thin Films* 26.C (Jan. 1999), pp. 23–49. ISSN: 1079-4050. DOI: 10.1016/S1079-4050(99)80005-2.

[7] H. Mansour et al. "Dislocation analysis of a complex sub-grain boundary in UO2 ceramic using accurate electron channelling contrast imaging in a scanning electron microscope". In: *Ceramics International* 45.15 (Oct. 2019), pp. 18666–18671. ISSN: 0272-8842. DOI: 10.1016/J.CERAMINT.2019.06.091.

[8] Batgerel Tumurbaatar et al. "A portable and computer-simulation analysis for the real-time measurement of the QCMD systems for the biomedical application". In: *Sensing and Bio-Sensing Research* 21 (Nov. 2018), pp. 75–81. ISSN: 2214-1804. DOI: 10.1016/J.SBSR.2018.08.004.

[9] Mattias Åstrand et al. "Understanding dose correction for high-resolution 50 kV electron-beam lithography on thick resist layers". In: *Micro and Nano Engineering* 16 (Aug. 2022), p. 100141. ISSN: 2590-0072. DOI: 10.1016/J.MNE.2022.100141. URL: https://linkinghub.elsevier.com/retrieve/pii/S2590007222000387.

[10] Barbara Horváth, Robin Schäublin, and Yong Dai. "Flash electropolishing of TEM lamellas of irradiated tungsten". In: *Nuclear Instruments and Methods in Physics Research, Section B: Beam Interactions with Materials and Atoms* 449 (June 2019), pp. 29–34. ISSN: 0168583X. DOI: 10.1016/j.nimb.2019.04.047.

[11] Miguel A. Gosálvez, I. Zubel, and Eeva Viinikka. “Wet etching of silicon”. In: *Handbook of Silicon Based MEMS Materials and Technologies*. Elsevier, Jan. 2020, pp. 447–480. ISBN: 9780128177860. DOI: 10.1016/B978-0-12-817786-0.00017-7.

[12] Taisiia Sikolenko et al. “Thickness control in electrogenerated mesoporous silica films by wet etching and electrochemical monitoring of the process”. In: *Electrochemistry Communications* 100 (Mar. 2019), pp. 11–15. ISSN: 13882481. DOI: 10.1016/j.elecom.2019.01.013.

[13] Jian Ming Ji et al. “Preparation of porous silicon substrate for protein microarray fabrication by double-cell electrochemical etching method”. In: *Fenxi Huaxue/ Chinese Journal of Analytical Chemistry* 41.5 (2013), pp. 698–703. ISSN: 18722040. DOI: 10.1016/S1872-2040(13)60653-2.

[14] *KOH Etching. (2022). Retrieved 14 June 2022, from https://cleanroom.byu.edu/koh.*

[15] Gustav Sundell et al. “Atom Probe Tomography for 3D Structural and Chemical Analysis of Individual Proteins”. In: *Small* 15.24 (June 2019). ISSN: 16136829. DOI: 10.1002/smll.201900316.

[16] Miguel A. Gosálvez, I. Zubel, and Eeva Viinikka. “Wet etching of silicon”. In: *Handbook of Silicon Based MEMS Materials and Technologies*. Elsevier, Jan. 2010, pp. 447–480. DOI: 10.1016/b978-0-12-817786-0.00017-7.

[17] Alexandre La Fontaine et al. “Interpreting atom probe data from chromium oxide scales”. In: *Ultramicroscopy* 159 (Dec. 2015), pp. 354–359. ISSN: 0304-3991. DOI: 10.1016/J.ULTRAMIC.2015.02.005.

A
Appendix 1

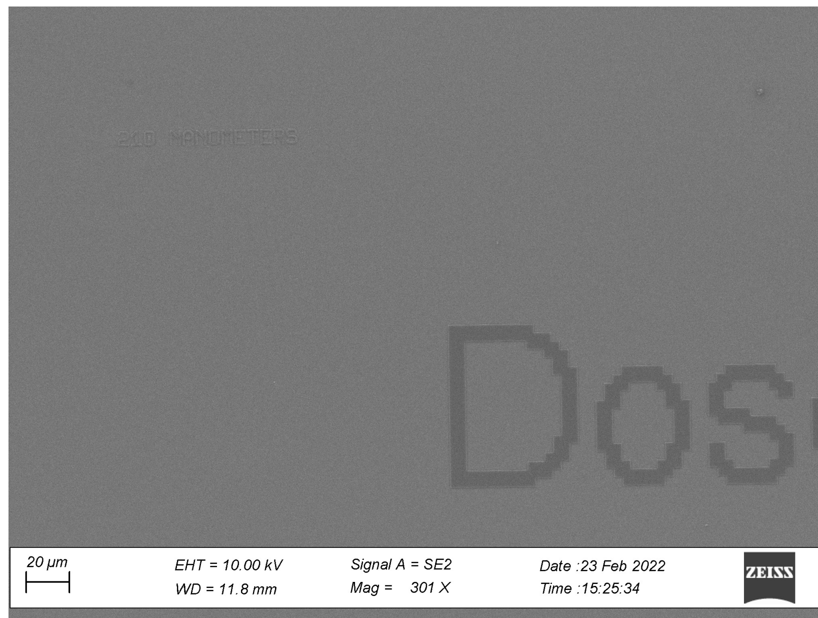

Figure A.1: 301X Magnification with measurement for 210 nm diameter pattern

Figure A.2: 433X Magnification with measurement for 210 nm diameter pattern

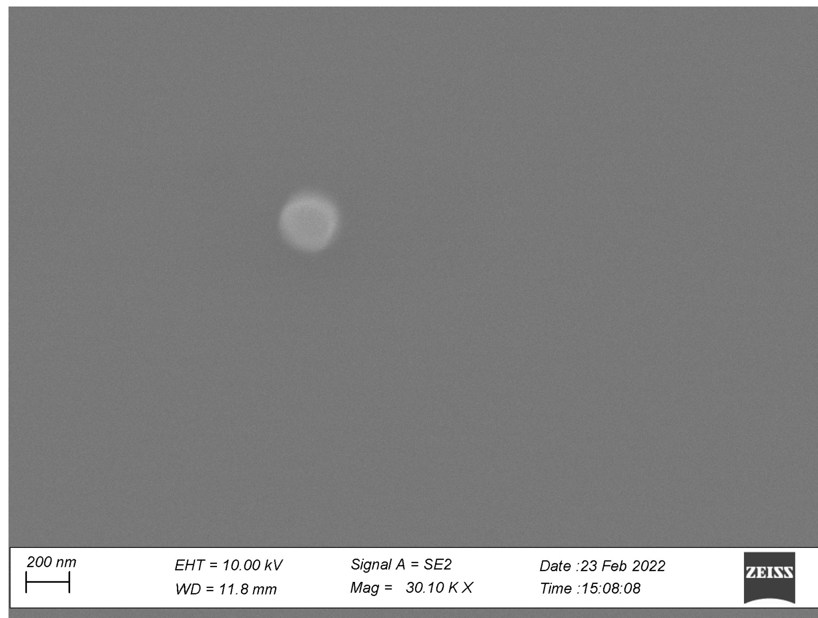

Figure A.3: 30KX Magnification with measurement for 210 nm diameter pattern

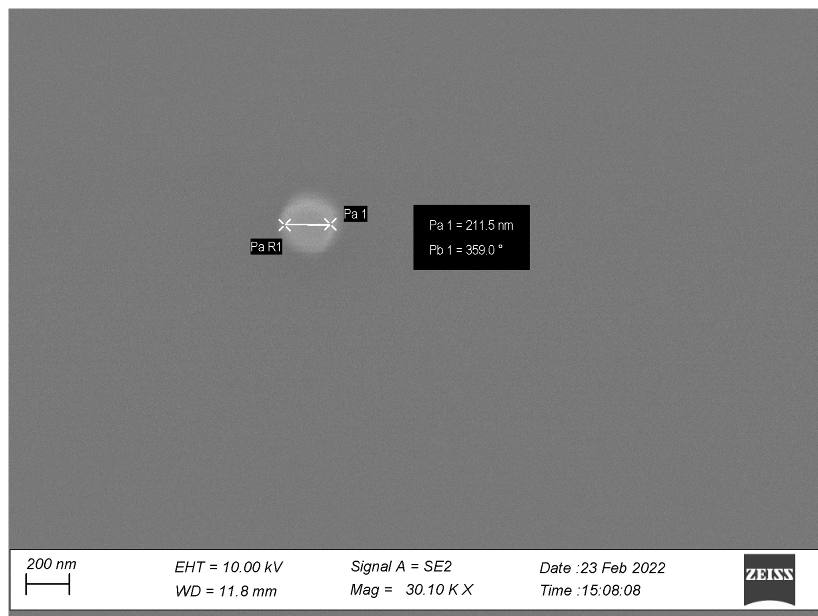

Figure A.4: 30KX Magnification with measurement for 210 nm diameter pattern

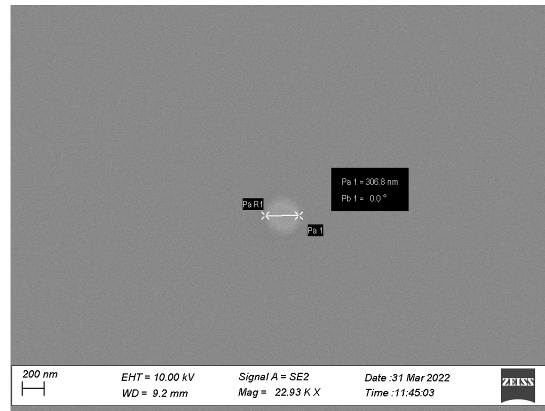

Figure A.5: 22KX Magnification with measurement for 250 nm diameter pattern at 550 dosage

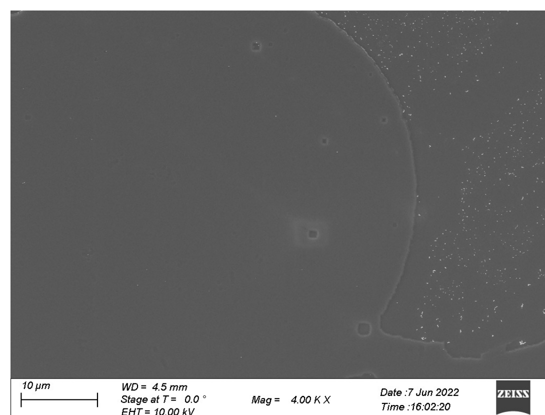

Figure A.6: Image of surface of silica on silicon chip after HF and KOH etching

Figure A.7: Image of 400 nm etched circle near 110 nm text

DEPARTMENT OF CHEMISTRY AND CHEMICAL ENGINEERING
DEPARTMENT OF MICROTECHNOLOGY AND NANOSCIENCE
CHALMERS UNIVERSITY OF TECHNOLOGY
Gothenburg, Sweden. www.chalmers.se

CHALMERS
UNIVERSITY OF TECHNOLOGY